

THESIS /  
REPORT

Miller,  
S.M.

DEVELOPMENT of PROBABILISTIC METHODOLOGIES  
for THREE-LEVEL LANDSLIDE ANALYSIS SYSTEM  
by

STANLEY M. MILLER

Progress Report for COOPERATIVE AGREEMENT  
INT-88295 with UNIVERSITY OF IDAHO

FS Contact: Carol Hammond  
Univ. Contact: Stanley Miller





Progress Report for  
Cooperative Agmt INT-88  
with University of Idaho  
FS Contact: Carol Hammer  
Univ Contact: Stanley Miller

January 19, 1989

College of Mines and  
Earth Resources

Beverly C. Holmes  
Assistant Station Director  
USDA-FS Intermountain Research Station  
324 25th Street  
Ogden, Utah 84401

University of Idaho  
Moscow, Idaho  
83843

RE: FY88 Progress Report for Co-op Research Agreement No. INT-88295

Office of the Dean  
208-885-6195

Please find enclosed five copies of the progress report referenced above. Some of the research results have been published in professional journals or in symposium proceedings, and thus, reprints of these articles are included as part of the progress report. It has been a pleasure working with Carol Hammond and Rod Prellwitz on this research work, and we look forward to continued interaction and cooperation.

Department of Metallurgical  
and Mining Engineering  
208-885-6376

Department of Geography  
208-885-6216

Feel free to contact Carol Hammond or me if you have any questions regarding our Co-op Agreement. My university telephone number is (208) 885-7977.

Department of Geology and  
Geological Engineering  
208-885-6192

Sincerely,

Stanley M. Miller, Assoc. Prof. of Geological Engineering

Idaho Mining and  
Mineral Resources  
Research Institute  
208-885-7989

P.D. &  
S.F. &  
A

Progress Report for USDA-FS

Cooperative Agreement No. INT-88295:

Development of Probabilistic Methodologies for  
Three-Level Landslide Analysis System

December, 1988

Department of Geology and Geological Engineering  
University of Idaho

1. Estimating Probability of Slope Failure for Level I and Level II

The probabilistic, computerized Level I Slope Stability Analysis (LISA) is currently in its final review and documentation phase. This analysis is based on a limit-equilibrium approach that uses the two-dimensional infinite slope model. A Monte Carlo simulation overlay allows for a suite of possible safety factors to be generated, from which a probability of slope failure can be estimated. Details of the procedure and the computer code are presented in the published article that comprises Attachment 1.

The Level II analysis focuses more on specific road locations and site evaluations than does the more reconnaissance-oriented LISA. Several types of slope failures associated with road construction are considered, including the following: infinite slope (for natural slopes located upslope from the road cut), cut slope, and fill slope. Stability of the road prism is evaluated using a probabilistic version of Cousins' stability charts/stability number approach, which is based upon an earlier deterministic version described by R. Prellwitz (1988, "SSIS" and "SSCHFS" -- Preliminary Slope Stability Analyses with the HP41 Programmable Calculator; USDA-FS Engr. Staff Publ. No. EM-7170-9, Washington, DC). The Monte Carlo simulation used in the Level II analysis to produce a distribution of possible safety factor values is similar to that used

in LISA, with the major exception of how the shear strength is handled. Because of the format of the limit-equilibrium equations used in Cousins' method, the cohesion and friction angle must be treated separately, rather than combining them into a single estimate of shear strength. Thus, we have proposed using a bivariate beta distribution to accommodate this dependent sampling of  $C$  and  $\phi$  for the Level II analysis. Work along these lines will continue into FY89, as we assist in developing the Level II slope stability code in conjunction with software developers Paul Swetik and Dave Hall at the Moscow, ID, Intermountain Research Station.

## 2. Guidelines for Sampling/Describing Input Values

At the Level I stage of slope stability analysis, the main sources of information used to estimate the input distributions for LISA are available resource inventories, geologic maps, soil maps, aerial photos, reference literature, and the experience and knowledge of the investigator. Some data collection on the ground is recommended, but we realize that only minimal effort will be expended on such endeavors at the Level I stage. The particular LISA input variables discussed below are: slope, soil depth, soil strength, and groundwater elevation. In general, at least 30 observations are needed to estimate reasonably the probability distribution of a given variable, although 10 to 12 observations can suffice if the user has field experience or knowledge of the variable.

Within each map unit or study area, slope measurements can be readily obtained from topographic maps (probably of the 7.5-min. USGS variety). To avoid bias and to obtain a representative sample, it is recommended that a stratified-random sampling scheme be used, whereby a regular grid is laid out over the map unit and a random location selected within each grid cell (box). At each location the slope is calculated by using the map scale and the contour interval. The slope values then are collectively plotted as a histogram, which leads to modeling of the probability distributional form of slope. Follow-up measurements of slope can be made on the ground using hand-held inclinometers, Brunton

compasses, or similar devices.

Soil depths may be inferred from soil maps or resource inventories compiled by the forest soil scientist, but in most cases some field work probably will be necessary to obtain appropriate distributional forms. Readily available locations for observing soil profiles include road cuts, ephemeral stream beds on valley sideslopes, and root-throw "pits" formed at the base of blown-down trees. The latter two sources often will only be accessible on foot. If limited recon hiking is justified, then a hand-held, impact-driven soil penetrometer should be taken along to make as many soil depth soundings as time permits. When a stratified-random sampling scheme is not feasible, then sampling can be done parallel to a road or along a given contour elevation(s). In this situation, soil depth readings can be taken at regular intervals deemed appropriate by the investigator or at random locations within regular cells along the sampling trace. Even if bedrock cannot be observed or probed at a given sampling site, the depth of soil cover observed should still be noted. Such "inequality" information provides useful input to modeling the probability distribution of soil depth.

At the Level I stage of investigation, little or no shear strength information will be available for soils. Thus, shear strength likely will be inferred indirectly from other soil properties that are available. Geotechnical reference literature contains some information on the anticipated cohesion and friction angles, given a certain category of soil as classified according to the engineering-oriented Unified Soil Classification (USC) scheme (ASTM standard D2487-85 or D2488-84). This should serve as a starting point for describing soil shear strength at Level I. If the district soil scientist has already established a regional classification based on the U.S. soil taxonomy (U.S. Soil Conservation Service) or other related system, then the soil types must be "translated" into the USC system if shear strength descriptions are to be derived. More specific guidelines for selecting cohesion and friction angle input distributions for LISA, given USC information, are being

developed. Field verification of USC identifications can be obtained by visual inspections of in-situ soils when the investigator is in the field making slope and/or soil depth measurements. In addition, further checks on cohesion and friction angle values are possible by conducting back-analyses of slope failures currently observed in the study area, if any. Using all of the above methods, the minimum objective of describing a range and/or shape of the probability distribution for  $C$  and  $\phi$  should be realized. Statistical dependence between  $C$  and  $\phi$  is accounted for within the LISA code via a user-defined correlation coefficient (see the discussion in Attachment 1).

The groundwater ratio input ( $D_w/D$ ) to LISA perhaps is the most difficult geotechnical variable to estimate at the Level 1 stage of analysis. Other than obvious indicators such as springs, seeps, boggy areas, and vegetation preference, there are no readily observable field features to help characterize water levels in the soil mantle. Topography can be used in a general way (e.g., hollows tend to concentrate groundwater, whereas ridge noses tend to disperse groundwater), but care should be taken against gross generalizations because local hydraulic properties often have the final say in the fluctuation of groundwater levels. However, it seems reasonable that a map unit with an abundance of hollow(s) area would have a groundwater height distribution more favorable to large values than one associated with a map unit primarily consisting of ridges or spurs. Soil profiles obtained by visual inspections of road cuts or test pits may provide indications (leaching or reducing environment) of historical maximum rises of groundwater. Back-analysis of slope failures in the study area also may give reasonable bounds to the local ground-water elevation at the time of failure. When attempting to formulate  $D_w/D$  probability distributions, the user should remember that this ratio is somewhat controlled by the soil depth. In particular, given all other factors equal, landforms with thin soils should have higher  $D_w/D$  ratios than those with deep soils.

### 3. Power-Curve Modeling of Shear Strength Data

Direct-shear test results from specimens of forest soils typical to the Pacific Northwest and northern Idaho were input to both linear and nonlinear regression analyses. The linear model is given by:

$$\tau = A(\sigma_n) + C$$

where:  $\tau$  = shear strength,

$\sigma_n$  = effective normal stress,

$A = \tan\phi$ , where  $\phi$  is the friction angle,

$C$  = apparent cohesion.

The power-curve model is given by:

$$\tau = A(\sigma_n)^B + C$$

where:  $\tau, \sigma_n$  = same as above,

$A, B, C$  = regression coefficients.

One of the major concerns of the linear model is that it tends to provide unrealistically high values of apparent cohesion in silty or sandy soils that are known to be cohesionless or nearly cohesionless. As a consequence, when such shear strength values are used in stability analyses of shallow soils or of soils experiencing high pore pressure (i.e., situations where very low normal stresses are present on the failure surface), the calculated safety factor will be unreasonably high. A curved failure envelope, such as that provided by the power-curve regression model, would be more representative in these situations.

As seen in Table 1, the power model provides nearly as good a fit, or better, than the linear model when using the mean absolute deviation (MAD) as a measure of goodness of fit. Also, for the SM soils (as per the Unified Soil Classif. scheme) the power model will yield considerably better estimates of shear strength at low normal stress values. Potential applications of this power-curve envelope warrant further research, given these promising results thus far.

Table 1. Example results of fitting regression models to shear testing data (units in psi,  $\phi$  in degrees).

Soil Type	Linear Model				Power Model			
	C	A (tan $\phi$ )	$\phi$	MAD	A	B	C	MAD
Linslaw Tie (SM)	2.93	0.772	37.7	0.834	2.014	0.736	0.032	0.697
Buck Crk. (SM)	1.80	0.843	40.1	0.242	1.557	0.825	0.000	0.272
Noti (SM)	0.34	1.059	46.6	1.001	0.987	1.003	0.000	0.939
Noti (SM)	2.41	0.814	39.1	0.293	1.834	0.768	0.000	0.349
CNF Alluvium (ML)	2.90	0.554	28.9	2.041	1.586	0.735	0.000	2.093
CNF Basaltic (ML)	1.33	0.454	24.4	0.867	0.932	0.801	0.000	0.942
CNF Quartzit (GM)	0.10	0.650	33.0	0.568	0.710	0.969	0.021	0.558
CNF Gneissic (SM)	0.72	0.656	33.3	0.259	0.905	0.908	0.000	0.305

#### 4. Basic Analysis of Groundwater Monitoring Data, Clearwater NF

Precipitation and groundwater monitoring continued at the Dan Lee Ridge site on the Clearwater National Forest of Idaho. Piezometer holes DH-2, DH-8, and DH-17, as well as a Sacramento precipitation gage and a lysimeter infiltration gage, were monitored with battery-powered data acquisition systems from October, 1987, through June, 1988. Hydrographs and a summary table of results are provided as Attachment 2. These results are similar to those obtained in recent years at the Dan Lee site.

#### 5. Evaluation of Groundwater Models

A doctoral student in hydrogeology at UI, Christian Petrich, has completed an initial evaluation/comparison of three commonly used groundwater flow models to determine their applicability to modeling groundwater conditions on steep hillslopes. Groundwater response has a major influence on slope stability in steep, forested lands. The three computer models investigated were: MODFLOW, PLASM, and UNSAT2, all of which are available in the public domain and all have been extensively used and tested. The results of Mr. Petrich's study are contained in Attachment 3.



#### 6. Using Historical Climate Records to Estimate Groundwater Behavior

An extreme-value statistical method is appropriate for estimating cumulative probability distributions for groundwater elevation fluctuations, provided that historical groundwater monitoring records are available in the study area. This is rarely the case, so a link must be established between historical precipitation/temperature data and subsequent groundwater behavior. Preliminary research efforts in this arena are presented in the journal article that comprises Attachment 4. Follow-up work has focused on numerical models that can be calibrated with a reasonable amount of field data and that will provide a rational, practical strategy for using historical climate data to "reconstruct" likely historical behavior in groundwater piezometric fluctuations (see Section 5 above).

#### 7. Cooperation with USBLM on 3DLISA Evaluation

Two meetings were held during 1988 with USBLM personnel in Eugene, Oregon, regarding common interests in slope stability assessments in steep forested terrain. The goal of the first meeting in June was to establish a cooperative research plan to evaluate the 3DLISA slope stability computer code under development at the Intermountain Research Station in Moscow, Idaho. Jerry Richeson of the USBLM agreed to hire a UI graduate student during summer 1988 to work on the project. A follow-up meeting was scheduled for September (later it was postponed until October); this meeting included an assessment of the summer efforts, continued project planning, and a discussion with Oregon State University researchers who are involved with the Oregon USBLM people on the Coastal Oregon Productivity Enhancement project (COPE). A summary of the UI's involvement, which was primarily the summer fieldwork, is given below.

The major goal of the summer fieldwork was to locate and describe representative headwall slope failures in the Coast Range that could be analyzed by the Burrough's 3-D block model, which is the basis for 3DLISA. Ideal characteristics of such failures include: distinct head

scarp, narrow block of failed material having a definable critical point at its lower end, and minimally disturbed sideslopes. Slope measurements were taken by standing in the critical point and using an inclinometer to estimate the fall-line angles (i.e., up and down the drainage) and the sideslope angles (i.e., the "alpha" angles measured perpendicular to the fall-line). The approximate length and width of the failure block were noted, and several soil-depth readings were taken up the sideslopes to allow for reconstruction of the pre-failure soil surface. A sketch of the drainage basin and any useful comments regarding vegetation type, soil type, etc., also were included.

A total of 13 headwall failures were described in detailed. Most were located by using information in earlier reports on slope stability in the Mapleton Forest District. Others were located by using eye-witness accounts from USDA-Forest Service and USBLM field personnel. The southern portion of the Mapleton district had the highest density of headwall failures. Only the most case-typical failures (appropriate for 3DLISA) were mapped and described. During the course of this fieldwork several observations were made that lead to the following conclusions:

- 1) the portable, impact-type penetrometer was heavy and difficult to carry in the field; a smaller version should be constructed;
- 2) in general, the lack of headwall buffer leave-areas contributes significantly to sideslope failures that occur subsequent to the block failures in the bottom of the drainage area;
- 3) the failure scars had a distinctly smooth, hyperbolic shape in lateral cross-section, apparently controlled by the underlying bedrock surface.

## **ATTACHMENT 1**

# ESTIMATING THE PROBABILITY OF LANDSLIDE FAILURE USING MONTE CARLO SIMULATION

By

Carol J. Hammond,<sup>1</sup> Stanley M. Miller,<sup>2</sup> Rodney W. Prellwitz<sup>3</sup>

## ABSTRACT

Evaluating the stability of variable landforms is important for resource allocation and timber sale planning by the USDA Forest Service. Much literature addresses hazard assessment of individual slopes, but little information is available concerning the evaluation of large areas. This paper describes a rational method for landslide hazard evaluation that considers natural variability, measurement error, and uncertainty in geotechnical input parameters. Monte Carlo simulation is used to estimate the frequency distribution of the safety factor of natural slopes for a given landform type using the infinite slope equation as the performance function. The probability of failure is taken as the relative frequency with which the calculated safety factors are less than or equal to 1. The simulation program is written for IBM-PC<sup>4</sup> and compatibles, includes a menu-driven user interface, and allows the choice of seven different input probability distributions to describe the natural variability and uncertainty of each input parameter. Correlations between parameters are incorporated when appropriate. Trial applications show good agreement between estimated (simulated) probabilities of failure and the percent of land surface area in failure as obtained from landslide inventories.

## INTRODUCTION

Many forest lands in the West are classified as potentially unstable. Unless carefully planned and executed, timber harvesting operations and road construction in these areas can accelerate mass failure and may cause significant impacts on soil productivity and water quality. Accurate assessment of potential landslide hazard early in the planning process is essential.

One approach for hazard assessment using geotechnical limit-equilibrium analysis relies on the calculation of a single safety factor value, which then is used to make a subjective landslide hazard assessment. For example, if the safety factor is greater than 1.7, the failure hazard might be considered as low; if it is between 1.2 and 1.7, the failure hazard might be considered as moderate; and if it is less than 1.2 the failure hazard might be considered as high (Schroeder, 1985). "Average", "most probable", or "conservative" values for each parameter in the limit-equilibrium equation are selected subjectively by geotechnical specialists. Computation of a single safety factor value, however, fails to express the variability and uncertainty in the estimation of the stability of a slope or landform. What is needed is to consider the natural variability and uncertainty of each input parameter in the analysis to obtain a distribution of possible safety factor values. A probability of failure, that is, the probability that the safety factor is less than or equal to one for a slope or landform, can then be assessed.

<sup>1</sup> Research Engineer, Intermountain Research Station, USDA-Forest Service, Moscow, Idaho 83843

<sup>2</sup> Assistant Professor of Geological Engineering, University of Idaho, Moscow, Idaho 83843

<sup>3</sup> Research Engineer, Intermountain Research Station, USDA-Forest Service, Missoula, Montana 59807

<sup>4</sup> The use of trade or firm names in this paper is for reader information only, and does not imply endorsement by the U.S. Department of Agriculture of a product or service.

Most probabilistic methods described in the literature look at variability of soil cohesion, angle of internal friction and/or ground water only. A closed form solution is derived for the mean and standard deviation of the safety factor which has an assumed distribution shape (usually normal, lognormal, or beta), and then a probability of failure is calculated (Chowdhury and Tang, 1987). The problem is that these methods do not consider variability of other important parameters, such as slope and soil depth. One reason all parameters are not considered as stochastic variables is because the calculus needed to evaluate the integrals resulting from the derivation of the probability distribution of safety factor would not be tractable. However, when analyzing large areas, as in resource planning, all of the input parameters have sufficient spatial variability and measurement uncertainty to warrant treatment as stochastic variables.

An alternative method to evaluate landslide hazard is Monte Carlo simulation, which allows many repeated calculations of safety factor. The histogram of these results provides an approximation of the probability distribution of safety factor. The probability of failure can be estimated from this simulated distribution.

This paper describes a micro-computer program that uses Monte Carlo simulation to help quantify the probability of landslides in residual or colluvial soils. The program is named *Level I Stability Analysis* (LISA). A Level I Stability Analysis is a relative landslide hazard evaluation for resource allocation. A Level II Analysis is evaluation of management impacts for comparing alternative transportation routes and timber harvest techniques for project planning. A Level III Analysis is evaluation of alternate road stabilization techniques at a specific critical site (Prellwitz, 1985).

#### Hazard vs. Risk

For the purpose of this paper we are defining hazard as the calculated probability of slope failure and risk as a measure of the socioeconomic consequences of slope failure. Two slopes may have the same estimated probability of slope failure, and therefore the same hazard. However, if a home or an anadromous fisheries stream lies below one of the slopes, the risks associated with failure of that slope are much greater than those associated with the other, where a failure would have far less impact. Risk analysis is beyond the scope of this paper.

#### MONTE CARLO SIMULATION

Monte Carlo simulation is useful for modeling an attribute that cannot be sampled or measured directly, but can be expressed as a mathematical function of properties that can be sampled or described. Safety factor fits this situation. If we want to predict a possible value of the safety factor, we take a possible value for each input variable and use the appropriate equation to calculate the corresponding value of safety factor. This is known as one Monte Carlo pass or iteration.

In Monte Carlo simulation we generate a considerable number of safety factor values, say 1000, by repeated random, independent samplings of a set of possible input values, and then calculate a corresponding safety factor value for each repeat. The set of possible input values is described by a probability distribution for each input parameter. The result is 1000 possible safety factor values that can be displayed as a histogram. The relative frequencies of these 1000 values are assumed to be representative of the frequencies we would have obtained if we had analyzed all possible combinations of the input variables. Thus, the relative frequency of the computed safety factors less than or equal to one is an estimate of the probability of occurrence of safety factors less than or equal to one in nature. We obtain the probability of failure by dividing the total number of passes into the number of calculated safety factor values less than or equal to one.



The number of passes required for the simulation study is the number necessary to provide consistent, stable results and is a function of the number of input stochastic variables, the shapes and ranges of the probability distributions for the input variables, and the performance function. Tests with LISA show that 1000 passes provide frequency histograms of safety factor that are not statistically different from frequency histograms generated with 10,000 passes for any case tested.

#### Details about LISA

In general, the operation of LISA is as follows:

- 1) The user selects a distribution shape and enters the values to describe that distribution for each parameter in the limit-equilibrium equation. The user may choose a constant value or a uniform, normal, lognormal, triangular, beta or histogram (relative frequency) distribution.
- 2) LISA generates a column of 1000 values for each parameter. The various procedures for simulating values from various distribution shapes are beyond the scope of this paper, but procedures can be found in Newendorp (1975), Iman & Shortencarier (1984), Rubinstein (1981), and Abramowitz and Stegun (1965). A frequency histogram of the 1000 values generated will closely match the shape of the distribution specified by the user for each parameter, but the 1000 values are generated in a random order (unless they are correlated to another input parameter).
- 3) Using the infinite slope equation for the limit-equilibrium analysis, LISA then calculates 1000 values of safety factor by taking one row of values at a time. We selected the infinite slope equation because it adequately analyzes the most common failure types found in the mountainous West—debris flows and debris avalanches characterized by the failure of a soil mantle that overlies a sloping bedrock surface (Prellwitz, et al, 1983). Also, the equation's simplicity allows for easy use in Monte Carlo simulation. Figure 1 and equation 1 show the form of the infinite slope equation used in LISA.

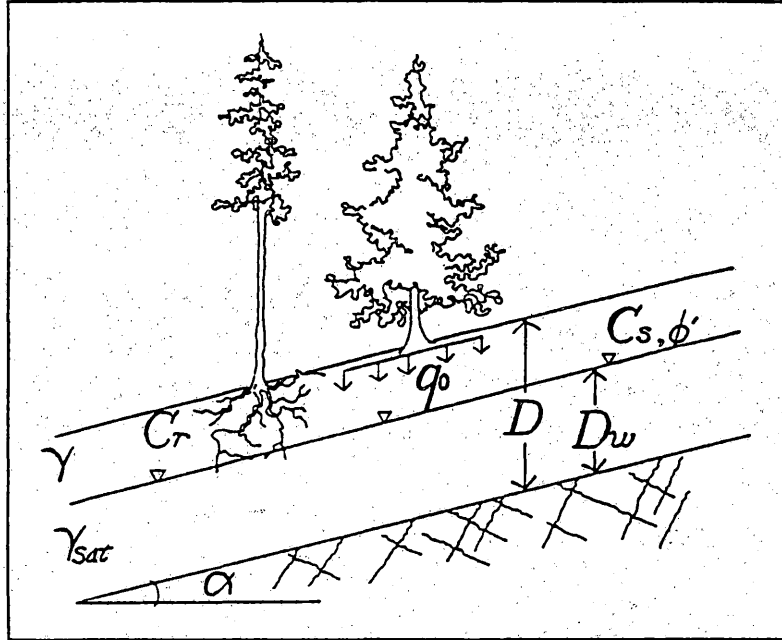
The user may then print or view the output file, which contains all of the input distributions used; the minimum, maximum, mean and standard deviation of the values simulated for each parameter; and a frequency histogram of the safety factor values simulated.

#### Correlation between Variables

Some of the stochastic variables in the infinite slope equation are not independent; the relationship between these variables must be accounted for to achieve a realistic simulation of safety factor values. The variables treated as dependent by LISA are soil cohesion and effective angle of internal friction, and soil unit weight and soil shear strength.

Soil cohesion and friction angle cannot be independent for they are two parameters describing a single straight line—the Mohr-Coulomb failure envelope. Figure 2 illustrates how treating soil cohesion and friction angle as independent variables could result in simulating unrealistic values of soil shear strength. Suppose one had three sets of shear strength tests on a particular soil, resulting in three Mohr-Coulomb failure envelopes. If LISA selected values of friction angle and cohesion independently, the highest value for each could be selected from the test data ( $C_{s3}$  with  $\phi'_1$ ), then the upper dashed failure envelope shown in figure 2 could result. Obviously this failure envelope is outside the possibilities given by the test data and would result in shear strength values that are too high. Similarly, shear strength values that are too low could also be simulated using  $C_{s1}$  with  $\phi'_3$  as illustrated by the lower dashed envelope in figure 2.

The scheme used to solve this problem in LISA is as follows: The user selects distributions for soil cohesion and friction angle, but LISA does not simulate values for them



$$SF = \frac{Cr + \tau}{\sin \alpha \cos \alpha [q_0 + \gamma(D - Dw) + \gamma_{sat}Dw]} \quad (1)$$

$$E[\tau] = E[C_s] + \sigma' n E[\tan \phi'] \quad (2)$$

$$Var[\tau] = Var[C_s] + \sigma' n^2 Var[\tan \phi'] + 2Cov[C_s, \tan \phi'] \quad (3)$$

$$\sigma' n = \cos^2 \alpha [q_0 + \gamma(D - Dw) + (\gamma_{sat} - \gamma_w)Dw] \quad (4)$$

$$Cov[C_s, \tan \phi'] = r * s(C_s) * s(\tan \phi') \quad (5)$$

where  $SF$  = safety factor

$Cr$  = tree root strength expressed as cohesion

$\tau$  = soil shear strength

$\alpha$  = slope of the ground surface

$q_0$  = tree surcharge

$\gamma$  = moist soil unit weight

$\gamma_{sat}$  = saturated soil unit weight

$D$  = total soil thickness

$D_w$  = saturated soil thickness

$C_s$  = soil cohesion

$\phi'$  = effective internal angle of friction

$\sigma' n$  = effective normal stress

$s(C_s)$  = standard deviation of  $C_s$

$s(\phi')$  = standard deviation of friction angle

$r$  = correlation coefficient between  $C_s$  and  $\phi'$

Figure 1. The infinite slope and related equations used in LISA.

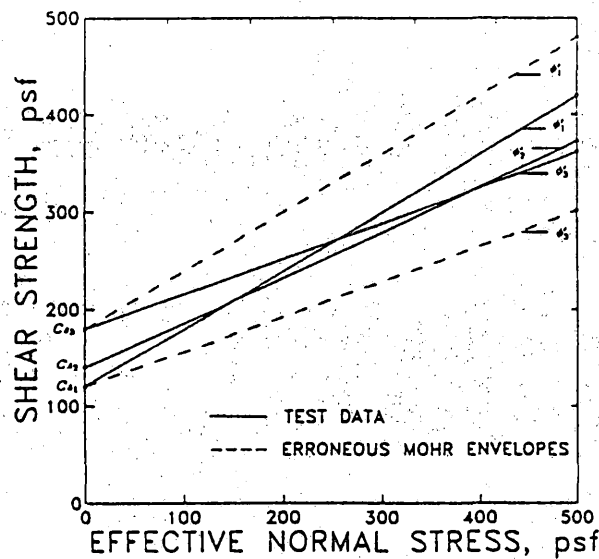


Figure 2. Independent sampling of  $C_s$  and  $\phi'$  could result in unrealistic values of shear strength as illustrated by the dashed lines.

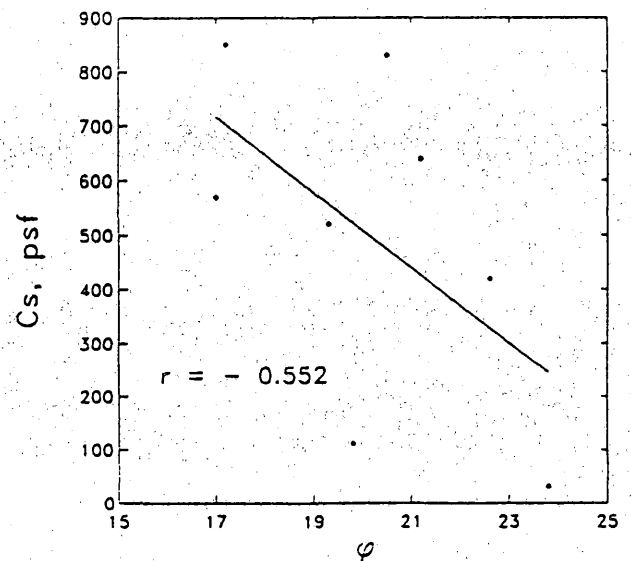


Figure 3. Illustration of the inverse relationship between  $C_s$  and  $\phi'$ .

directly. Rather, the mean and standard deviation of  $C_s$  and  $\phi'$  are calculated and used, along with effective normal stress, to calculate the mean or expected value of shear strength ( $E[\tau]$ ) and the variance of shear strength ( $Var[\tau]$ ). For each Monte Carlo pass, LISA first simulates values for each of the other input variables and calculates the effective normal stress (equation 4). The mean and variance of  $\tau$  then are calculated using equations 2 and 3. A value of  $\tau$  then is simulated from a lognormal distribution with mean  $E[\tau]$  and variance  $Var[\tau]$ . The lognormal distribution is used to prevent simulating negative shear strength values.

Although there exists some contradiction in the literature, soil cohesion and friction angle are generally considered to be inversely related, as illustrated in figure 3. Correlation coefficient ( $r$ ) values of -0.2 to -0.85 have been reported (Cherubini, et al, 1983). This inverse relationship is accounted for by the covariance term of equation 3 in the calculation of the variance of soil shear strength. Comparing figure 4a with 4b illustrates how larger negative values of  $r$  act to reduce the variance of shear strength. The user inputs a value for the correlation coefficient and LISA calculates covariance using equation 5. Apparent soil cohesion due to capillary suction is not inversely correlated with effective friction angle. In this case  $r$  may be taken as 0.

The second relationship, that between soil unit weight and soil shear strength, recognizes the angle of internal friction of soil increases as relative density (and unit weight) of the soil increases. For cohesive soils, cohesion also may increase with increasing unit weight, if the factors causing the higher unit weight of the soil also cause overconsolidation of the soil. Therefore, there is a direct relationship between soil shear strength and unit weight. LISA handles this relationship very simplistically by using the same random number to sample from the distributions of soil unit weight and soil shear strength. Therefore, when a high value is sampled for unit weight, a high value is sampled for soil shear strength to model the desired proportional relationship.

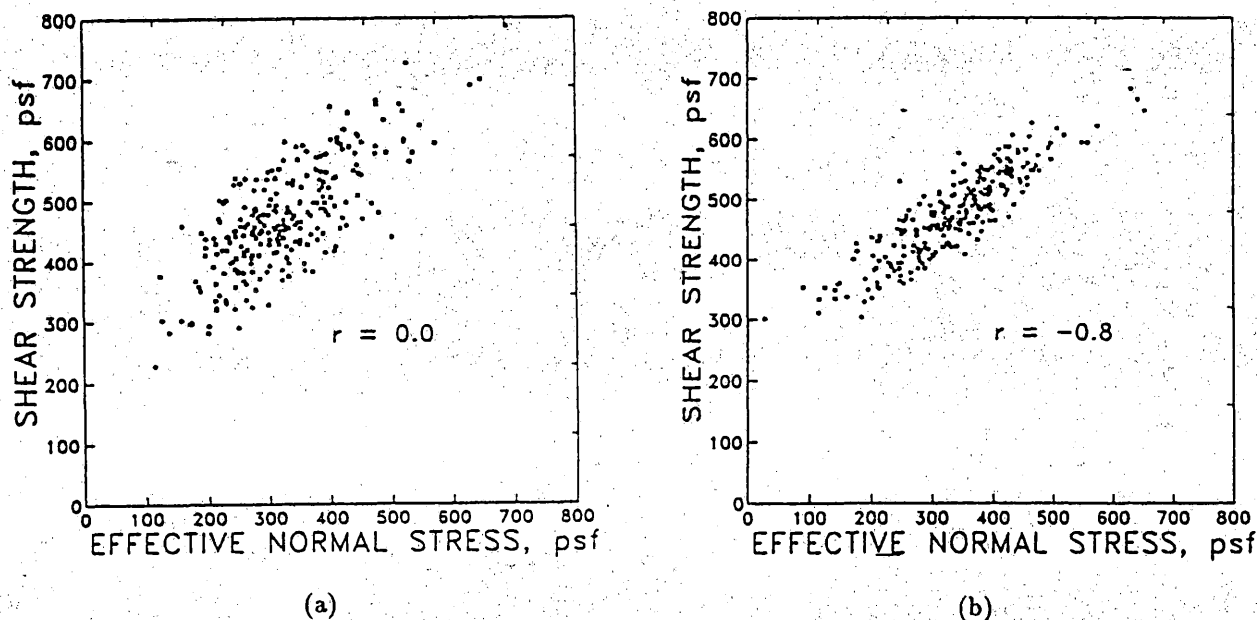


Figure 4. Reduction in the variance of soil shear strength considering the correlation between  $C_s$  and  $\phi'$ .

#### Simulating groundwater values

To prevent simulating a groundwater depth ( $D_w$ ) value that is not consistent with the simulated soil depth ( $D$ ) on any given pass, LISA simulates a value of groundwater-soil depth ratio ( $D_w/D$ ) from a distribution defined by the user. LISA then multiplies the simulated value of  $D_w/D$  by the simulated value of  $D$  to obtain a value of  $D_w$  to use in equations 1 and 4. LISA does not correctly calculate safety factor if  $D_w/D$  values are negative or greater than 1, so effective stress due to soil suction and artesian pressures cannot be analyzed.

#### INTERPRETATION OF PROBABILITY OF FAILURE

The probability of failure should be interpreted strictly as the total number of Monte Carlo passes divided into the number of Monte Carlo realizations of safety factor (i.e. calculated values of safety factor) with values less than or equal to one. It is the relative frequency with which possible values of safety factor are less than or equal to one.

If sufficient data are available, the probability distribution of each input parameter represents the areal distribution of that parameter across the landform. Therefore, the probability of failure can be thought of as the expected percent area of the landform involved in failure during the time period appropriate to the analysis. Without much data, the input distributions represent one's uncertainty about the parameter as well as one's best guess about their spatial distributions. Therefore, because of the two-dimensional nature of the infinite slope analysis, the estimated probability of failure is the likelihood that any possible cross-section through the slope would be analyzed as being unstable. The probability of failure also can be perceived as the probability of landslide occurrence if the area analyzed is small enough (i.e one slope or one drainage) so that only one failure could occur within the area.

Landslide inventories provide the best means to verify whether the estimated probability of failure values are reasonable. Landslide inventories traditionally have been used to assess relative hazard by drawing the inductive conclusion that landslides will occur again in areas where they have occurred previously. Therefore, areas with many inventoried landslides should have a high probability of failure as predicted by LISA. When considering the percent of the land area involved in landslides, we must realize that these "high" probabilities of failure may actually occur on a small portion of the landscape. Published landslide inventories report values on the order of 0.5 percent to 15 percent of the area inventoried (Ice, 1985). If the input distributions are mostly best guesses rather than estimated from actual data, there may only be a relative comparison between LISA-predicted probabilities of failure and percent-areas in slope failure. As with any computer program, "garbage in = garbage out". If the input distributions do not describe realistically the values and distributions of parameters on the ground, then the simulated probability of failure will not provide a realistic measure of landslide hazard.

LISA does not simulate the number of failures that might occur or the size of the failures on a particular landform. Therefore, LISA cannot be used to estimate volumes of sediment delivered to a stream, or to determine if sediment will reach a stream. Size and numbers of failures could be simulated if sufficient inventory data were available to estimate the distributions of landslide size and number that could be expected for certain landforms and/or soil/rock types.

#### Interpretation of Groundwater Probabilities

The groundwater condition (in particular, the height of the phreatic surface) in a natural slope is transient. Thus, for LISA to provide realistic assessments of landslide hazard, the groundwater height input distribution should have a temporal flavor. In general, the probability that the yearly maximum groundwater level will rise high in the soil profile would increase as the length of time under consideration increases, because the probability of having a major rain storm, rapid snow melt, or rain-on-snow event would also increase (Miller, 1987). In future investigations, we will attempt to use the groundwater distribution to incorporate time into the probability of failure estimate. For example, if we assume the groundwater distribution applies to a 20-year time period, then the probability of failure would also apply to a 20-year time period.

Unfortunately, neither the precipitation data nor the groundwater response data usually are available to do a detailed time-history analysis and we are forced to make subjective estimates of groundwater response in a "major" storm event. We interpret the groundwater distribution used in LISA as representing the spatial distribution of the maximum groundwater ratios expected across the landform during a major storm. For example, a landform with a concave shape may have 60 percent of the area in which the groundwater flowlines are roughly parallel, and 40 percent of the area in which groundwater flowlines converge (i.e. in a defined drainage). This might be represented by a frequency histogram with two cells; one cell with  $Dw/D$  ratios between 0.3 and 0.5 and a 60-percent frequency, the second with  $Dw/D$  ratios between 0.7 and 1 and a 40-percent frequency. The probability of failure would then be interpreted as a conditional probability of failure given that the "major" storm will occur. If a major storm does not actually occur, the probability of failure would be less than that estimated by LISA. Conceptually, the groundwater distributions would be different for different landforms depending on whether groundwater flowlines tend to converge or diverge.

#### USE OF THE PROBABILITY OF FAILURE

The probability of failure can be used qualitatively to make relative comparisons to identify areas with high probabilities of failure that should be targeted for additional anal-



ysis. The probability of failure also can be used more quantitatively in a risk analysis, such as an expected monetary value (EMV) decision analysis. Research efforts are continuing in this area.

Often in land management planning, one has to make subjective judgements about what probability of failure is acceptable. Interpretation of the probability of failure as the percent area expected in failure can help geotechnical specialists recommend to land managers what probability of failure is excessive. However, it would be better to have the consequences of failure identified with an estimate of the quantity of material that may impact downslope lands or streams.

We encourage users not to report a single value for probability of failure because that tends to imply precision in the results. Rather we encourage users to do sensitivity analyses with LISA, changing the shape and values describing the input distributions over realistic ranges to see how the probability of failure is affected. The range of values obtained should then be reported.

Used as an iterative tool, LISA can help the user document personal judgements and observations about an area, communicate them to other geotechnical specialists, and help identify factors critical to landslide hazard assessment in a given area.

#### EXAMPLE APPLICATIONS

##### Mount Hood National Forest-Lake Branch Study Area

The Lake Branch Study Area is located about 10 miles northwest of Mt. Hood in Oregon. The study area was divided by the Forest geologist into 4 soil units A through D, and arbitrarily subdivided into 26 polygons (Figure 5). Each polygon was evaluated by

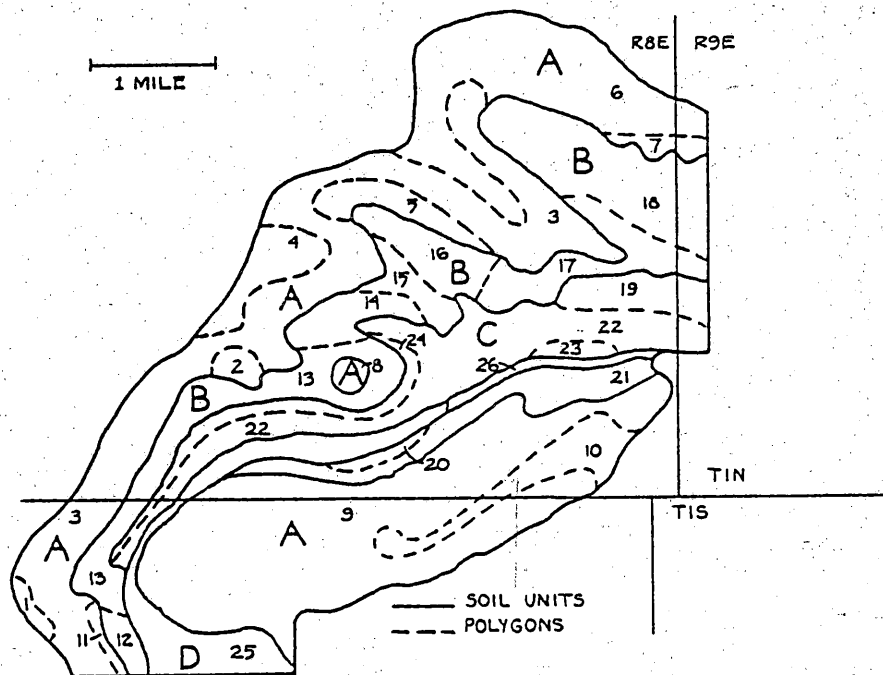


Figure 5. Lake Branch Study Area.

the authors using information provided by the Forest geologist. Triangular distributions for soil depth,  $Dw/D$ , dry unit weight and water content were estimated for each soil type. Normal distributions for effective internal angle of friction and soil cohesion were estimated using values from the literature correlated to the unified soil classification for each soil type. Triangular distributions for ground slope were estimated for each polygon by measurements on a 1:15,840 scale topographic map. Frequency histogram distributions for root strength were obtained by estimating the percent of land area within each polygon that fell into one of three categories—clearcut (CC), mixed shrubs and timber (P-partial cut), and uncut timber canopy (U-uncut). A range of root strength values for each category were estimated from Simons, Li and Ward (1978). The input distributions used are shown in Table 1. As an example, the printout for the LISA simulation of Polygon 17 is shown in figure 6.

Table 1. Input distributions used in the Lake Branch Study.

SITE FILE		SOIL TYPE			
		A	B	C	D
Soil Depth		2 5 6	3 9 10	3 13 15	10 30 50
Slope	A TRIANGULAR distribution for each polygon {i.e., T[min,apex,max]}				
qo					
		CC = % land area in each polygon that is ClearCut. P = % land area in each polygon that is Partial cut. U = % land area in each polygon that is Uncut.			
Cr					
MATERIAL FILE		SOIL TYPE			
		A	B	C	D
USC		GM TO GP	SC TO SMu	SC TO CL	GW TO GP
$\gamma_d$		T[100,105,115]	T[85.95,105]	T[75,85,95]	T[100,105,115]
% w		T[5,10,15]	T[10,15,18]	T[12,20,25]	T[5,10,15]
$\phi'$		N[32,2]	N[28,5]	N[25,5]	N[34,2]
Cs (psf)		N[40,10]	N[150,50]	N[200,50]	N[20,5]
r		0	0	0	0
GROUNDWATER FILE		SOIL TYPE			
		A	B	C	D
		T[0,.2,.5]	T[0,.4,1]	T[0,.4,1]	T[0,.6,1]; poly 25 T[0,.2,.6]; poly 26

# Estimating the Probability of Landslides using Monte Carlo Simulation by Carol J. Hammond, Stanley M. Miller, and Rodney W. Prellwitz Page 10

LEVEL I STABILITY ANALYSIS -- INFINITE SLOPE EQUATION  
November 1987

PROBABILITY OF SLOPE FAILURE

MOUNT HOOD NF -- LAKE BRANCH STUDY AREA -- POLYGON 17

OPERATOR : CAROL  
DATE & TIME : 01-21-2022 19:33  
MAP UNIT : MHLAKE.MFU  
# OF ITERATIONS: 1000

Random number seed 612667833736068.

INPUT DATA  
=====

SITE FILE : POLY17.SIT

SOIL DEPTH (ft) TRIANGULAR.  
MIN.: 3.00 APEX: 9.00 MAX.: 10.00  
SLOPE (%) TRIANGULAR.  
MIN.: 50.00 APEX: 70.00 MAX.: 75.00  
TREE SURCHARGE (pcf) HISTOGRAM. 4 CELLS  
MIN MAX PERCENT  
.00 10.00 33.30  
10.00 30.00 33.30  
30.00 50.00 .00  
50.00 70.00 33.30  
ROOT COHESION (pcf) HISTOGRAM. 4 CELLS  
MIN MAX PERCENT  
.00 40.00 33.30  
40.00 60.00 33.30  
60.00 80.00 .00  
80.00 100.00 33.40

MATERIAL FILE : POLY17.MTL

FRICTION ANGLE (deg) NORMAL.  
MEAN: 29.00 S.D.: 5.00  
SOIL COHESION (pcf) NORMAL.  
MEAN: 150.00 S.D.: 50.00  
DRY DENSITY (pcf) TRIANGULAR.  
MIN.: 85.00 APEX: 95.00 MAX.: 105.00  
MOISTURE CONTENT (%) TRIANGULAR.  
MIN.: 10.00 APEX: 15.00 MAX.: 18.00  
SPECIFIC GRAVITY OF SOLIDS 2.660  
R (tan PHI, Cs) .000

GROUNDWATER FILE : POLY17.HYD

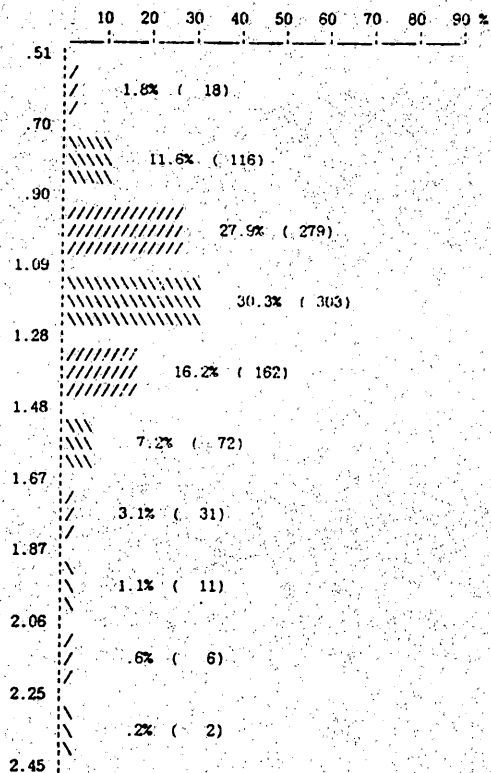
Dw/D ratio TRIANGULAR.  
MIN.: .00 APEX: .40 MAX.: 1.00

DESCRIPTIVE STATISTICS OF GENERATED DATA  
=====

	MIN	MAX	MEAN	S.D.
FACTOR OF SAFETY	.51	2.45	1.17	.27
SOIL DEPTH (ft)	3.06	9.96	7.31	1.55
SURFACE SLOPE (%)	51.16	74.49	64.90	5.22
TREE SURCHARGE (pcf)	.03	69.86	28.31	23.78
ROOT COHESION (pcf)	.04	99.99	53.72	29.61
FRICTION ANGLE (deg)			28.00	5.00
SOIL COHESION (pcf)			150.00	50.00
DRY DENSITY (pcf)	85.19	104.28	94.99	4.22
MOIST DENSITY (pcf)	95.58	120.91	108.64	5.00
SAT. DENSITY (pcf)	115.56	127.48	121.68	2.64
MOISTURE CONTENT (%)	10.12	17.89	14.38	1.67
DW/D RATIO	.00	.99	.46	.21
SHEAR STRENGTH (pcf)	156.06	746.38	394.26	89.41

Probability of failure = .267

FACTOR OF SAFETY FREQUENCY HISTOGRAM



MIN	Factor of Safety	.51
MAX	Factor of Safety	2.45
MEAN	Factor of Safety	1.17
MEDIAN	Factor of Safety	1.14

Figure 6. Example LISA printout.

The probabilities of failure estimated by LISA were compared to the percent of the land area within each polygon with mass failures according to the Forest geologist's landslide inventory. The landslide area inventoried included both natural failures and failures resulting from timber harvest, but did not include road related failures since LISA does not adequately analyze these. The results of the analysis are shown in Table 2.

Table 2. RESULTS

POLYGON	SOIL	AREA (acres)	INVENTORIED LANDSLIDE AREA (acres)	FRACTION OF AREA IN LANDSLIDES	LISA PROBABILITY OF FAILURE	CORRE- LATION
1	A	39	0	0.000	0.868	POOR
2	A	46	0	0.000	0.622	POOR
3	A	1840	40	0.022	0.019	GOOD
4	A	322	0	0.000	0.000	GOOD
5	A	176	0	0.000	0.000	GOOD
6	A	1052	0	0.000	0.000	GOOD
7	A	110	0	0.000	0.000	GOOD
8	A	41	0	0.000	0.029	MODERATE
9	A	2080	12	0.006	0.106	MODERATE
10	A	367	5	0.013	0.000	MODERATE
11	A	45	23	0.509	0.000	POOR
12	B	59	23	0.395	0.002	POOR
13	B	483	49	0.101	0.070	GOOD
14	B	144	3	0.022	0.036	GOOD
15	B	242	0	0.000	0.007	GOOD
16	B	292	5	0.018	0.003	MODERATE
17	B	314	4	0.014	0.279	MODERATE
18	B	548	1	0.012	0.002	MODERATE
19	B	108	4	0.037	0.136	MODERATE
20	B	92	0	0.000	0.000	GOOD
21	B	456	18	0.040	0.035	GOOD
22	C	940	53	0.056	0.085	GOOD
23	C	102	0	0.000	0.033	MODERATE
24	C	333	0	0.000	0.291	POOR
25	D	568	12	0.012	0.000	MODERATE
26	D	44	0	0.000	0.000	GOOD

One half of the polygons show good agreement between the probability of failure estimated by LISA and the actual decimal fraction of land area in failure. This includes 7 polygons for which the probability of failure was estimated at 0.000 and no failures are observed. Nine of the polygons show marginal agreement. The reasons for the discrepancies could be many, ranging from incomplete inventory of landslides to inaccurate descriptions of soil thickness and groundwater conditions. More accurate results would be obtained if probability distributions for soil depth and groundwater height were estimated for each polygon, rather than the same distributions used for all polygons within each soil type. Five of the polygons, 1,2,11,12, and 24, show poor correlation with LISA results. Polygons 1, 2, and 24 have very steep slopes, so that LISA simulated a very high probability of failure even though no failures exist. It is likely that groundwater and/or soil thicknesses are less than used in the simulation. LISA predicted no probability of failure for polygons 11 and 12 which have a fairly high fraction of land area in failure. But the failure area is

due to two large earthflows that initiated in polygon 3 and flowed downslope into 11 and 12, as well as 13. These earth flows are large enough that they probably have unique conditions and should be analyzed as separate polygons. Overall, the results look reasonable considering the number of estimates that were made for the input distributions.

#### **Use of LISA to Evaluate Changes in Probability of Failure due to Timber Harvest.**

Two parameters that are critical to slope stability change when timber is harvested—maximum ground water rise and tree root strength. Gray and Megahan (1981) report an approximate 100-percent increase in the maximum piezometric height during spring snow melt in two small basins after they had been clearcut, even though the snow water equivalent remained the same or decreased. This increase was attributed to an increase in available water due to a reduction in evapotranspiration after timber harvest. Tree root strength (expressed as a cohesion,  $C_r$ ) declines after timber harvest (Greenway, 1987). Root strength is considered to be at a minimum 5 to 12 years after harvest, by which time regrowth causes it to begin increasing again. Large storms during the period of minimum root strength can have a detrimental effect on slope stability.

Therefore the effects of timber harvest on natural slope stability can be evaluated with LISA by increasing the probability of high groundwater and by reducing the values of tree root strength. Such an analysis was attempted by Wooten (1987) on the Gifford Pinchot National Forest in south-central Washington. An unstable area, as evidenced by naturally occurring debris flows and earth slumps, was targeted for timber harvest. Wooten estimated ground slopes, soil shear strengths and soil depths by a field reconnaissance of the area. Root strength values were estimated from the literature. Estimates of possible groundwater heights resulting in failure were obtained by back-calculating the groundwater ratio  $D_w/D$  at a safety factor of 1 for the reconstructed original ground profile of a recent debris flow. A distribution around this back-calculated  $D_w/D$  value was used for the uncut condition. The probability of high groundwater was increased for the clearcut condition.

Wooten found that the probability of failure increased from 0.25 for the uncut (natural) condition to 0.58 for the clearcut condition. The inventory of existing landslides in the area showed that 0.25 was much higher than the percent surface area in failure. Therefore, Wooten elected to use this as a relative landslide hazard analysis, concluding that the occurrence of slope failure could increase by about 2 fold above natural levels if the timber is harvested and a "major" storm event occurs. This analysis then gives managers the ability to evaluate the risks associated with cutting the area.

#### **FUTURE WORK**

The Level II stability analysis is currently being programmed. The Level II model will use Cousins estimated safety factor (Cousins, 1978) in the Monte Carlo analysis to estimate the probability of failure of cut and fill slopes. We anticipate a working version will be available in about one year.

#### **ACKNOWLEDGEMENTS**

We must give special thanks to our computer programmers Paul Swetik and David Hall. Without their efforts LISA would not yet be a reality.

We also wish to thank Deborah Schnell for drafting the figures in this paper.



#### REFERENCES

- Abramowitz, A.; Stegun, I. A., eds. 1965. Handbook of Mathematical Functions with Formulas, Graphs, and Mathematical Tables. Dover.
- Benjamin, J. R.; Cornell, C. A. 1970. Probability, Statistics, and Decision for Civil Engineers. McGraw Hill, New York.
- Cherubini, C.; Cotechia, V.; Renna, G.; Schiraldi, B. 1983. The use of bivariate probability density functions in Monte Carlo simulation of slope stability in soils. Proc. of the Fourth Int. Conf. on Applications of Statistics and Probability in Soil and Structural Eng., Pitagora, France, p. 1401-1411.
- Chowdhury, R. N.; Tang, W. H. 1987. Comparison of risk models for slopes, in Reliability and Risk Analysis in Civil Engineering. Proc. of the Fifth Int. Conf. on Appl. of Statistics and Probability in Soil and Structural Eng., Vancouver, B.C. Canada, Vol. 2, p. 863-869.
- Cousins, B. F. 1978. Stability charts for simple earth slopes. ASCE, J. Geotechnical Eng. Div., Vol. 104, No. GT2, p. 267-279.
- Gray, D. H.; Megahan, W. F. 1981. Forest vegetation removal and slope stability in the Idaho batholith. USDA Forest Service, Intermountain Research Station. Research Paper INT-271.
- Greenway, D. R. 1987. Vegetation and slope stability. in Slope Stability, M. G. Anderson and K. S. Richards, eds., John Wiley and Sons.
- Ice, G. G. 1985. Catalog of landslide inventories for the northwest. National Council of the Paper Industry for Air and Stream Improvement, Inc. (NCASI) technical bulletin no. 456.
- Iman, R. L.; Shortencarier, M. J. 1984. A FORTRAN 77 program and user's guide for the generation of latin hypercube and random sample for use with computer models. Sandia National Laboratories.
- Newendorp, P. D. 1975. Decision Analysis for Petroleum Exploration. PennWell Publishing Co., Tulsa, Oklahoma.
- Prellwitz, R. W. 1985. A complete three-level approach for analyzing landslides on forest lands. Proceedings of workshop of slope stability: problems and solutions in forest management. USDA Forest Service, Pacific Northwest Forest and Range Experiment Station, General Technical Report PNW-180, p. 94-98.
- Prellwitz, R. W.; Howard, T. R.; Wilson, W. D. 1983. Landslide analysis concepts for management of forest lands on residual and colluvial soils. Transportation Research Record 919, p. 27-36.
- Rubenstein, R. Y. 1981. Simulation and the Monte Carlo Method. John Wiley and Sons. New York.
- Schroeder, W. L. 1985. The Engineering approach to landslide risk analysis. Proceedings of a workshop on slope stability: problems and solutions in forest management. USDA Forest Service, Pacific Northwest Experiment Station. GTR PNW-180.
- Simons, D. B.; Li, R. M.; Ward, T. J. 1978. Mapping of potential landslide areas in terms of slope stability. Colorado State Univ. Contract No. 16-712.01-CA for USDA Forest Service, Rocky Mountain Forest and Range Experiment Station.
- Wooten, R. M. 1987. Jackstraw Timber Sale. Unpublished in-service geologic report, USDA Forest Service, Gifford Pinchot National Forest, Zone II Engineering, Cook, WA.

## **ATTACHMENT 2**

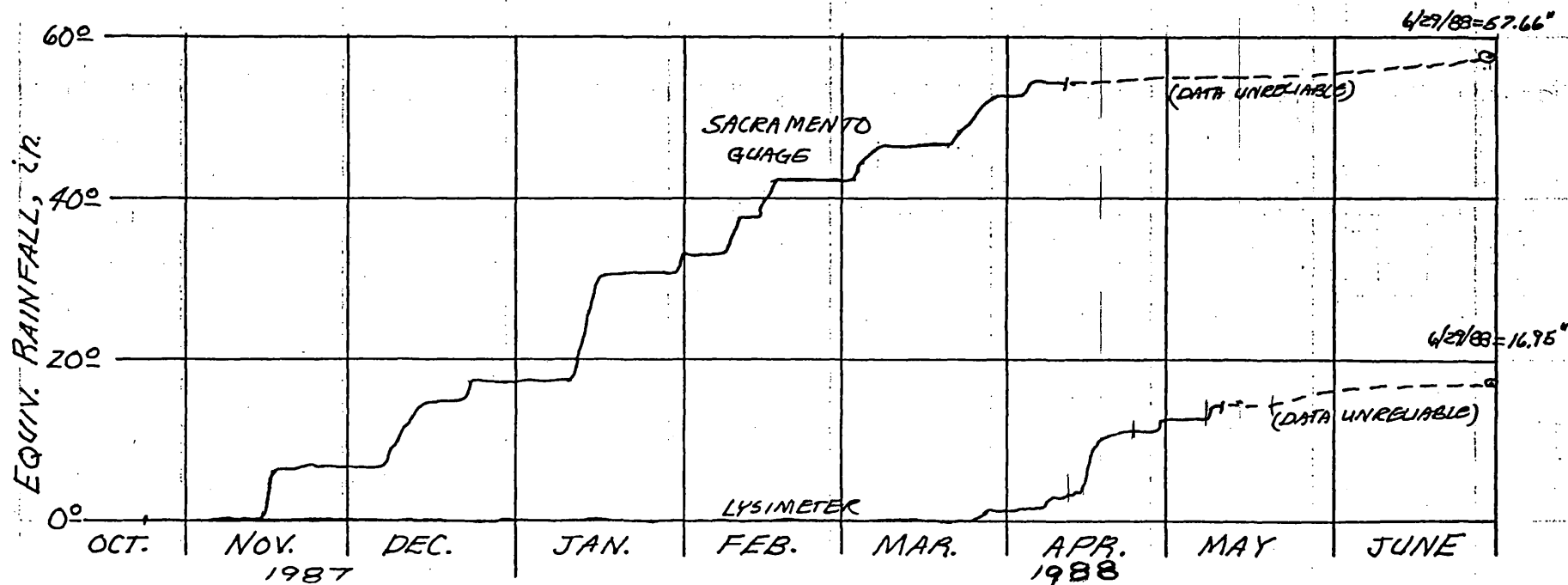
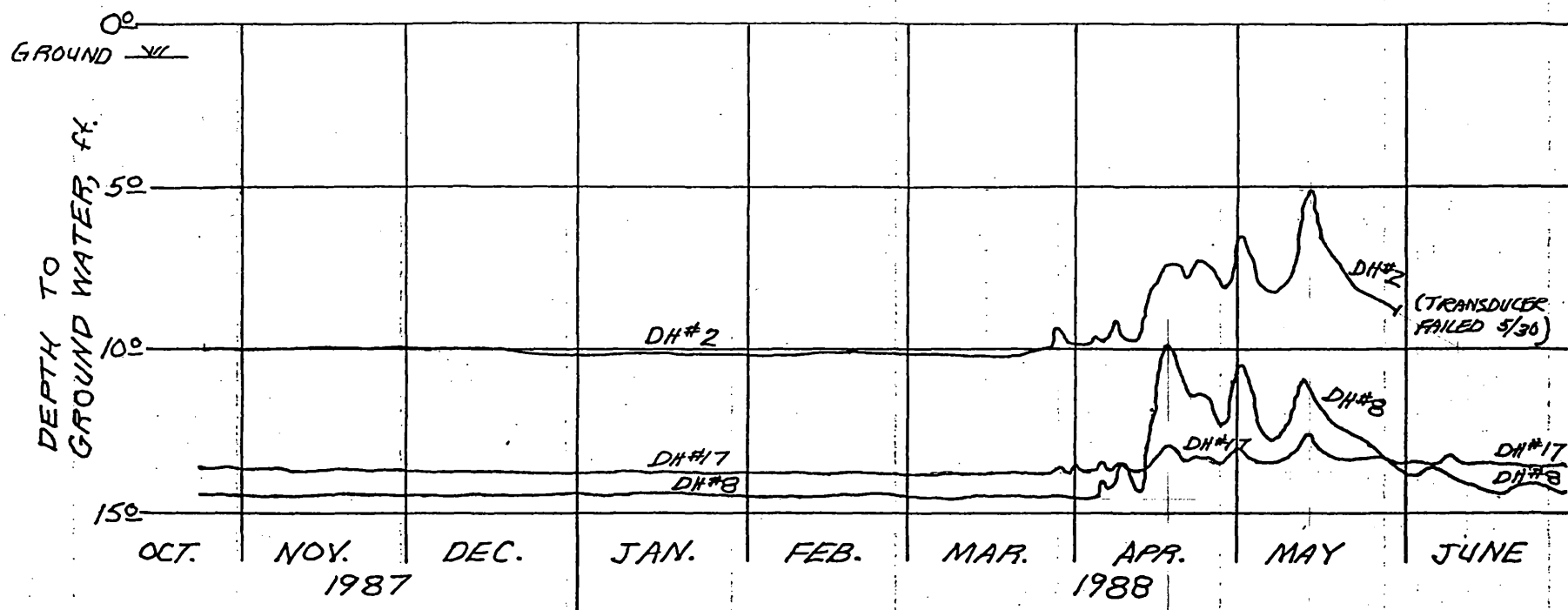
Dan Lee Site -- 1988

	Piezometer Holes		
	<u>DH-2</u>	<u>DH-8</u>	<u>DH-17</u>
Maximum net rise in piezometric level (ft.)	5.1	4.7	1.2
Seasonal accumulation of equiv. precip. when maximum piez. level observed (in.)	55*	54*	55*
Seasonal accumulation of water infiltration (in.):			
-- when maximum piez. level observed	14.8	10.2	14.8
-- six days prior to maximum observed piez. level	12.6	3.1	12.6
-- six days after maximum observed piez. level	15.2*	11.1	15.2*
Time interval of significant rise in piez. level (days)	3/27-6/15* = 80	4/5-6/15 = 71	4/5-6/22 = 78

---

\* Approximate or estimated.

# DAN LEE WATERSHED, CLEARWATER NATIONAL FOREST, IDAHO



## **ATTACHMENT 3**



**OVERVIEW OF SELECTED GROUND WATER FLOW MODELS WITH  
APPLICATION TO STEEP SLOPES**

**Christian R. Petrich**

**September, 1988**

## TABLE OF CONTENTS

I.	INTRODUCTION .....	1
	1.1 Purpose of Project .....	1
	1.2 Selection of Models for Comparison ...	1
II.	BACKGROUND .....	2
III.	DESCRIPTION OF MODELS .....	3
	3.1 MODFLOW .....	3
	3.2 PLASM .....	5
	3.3 UNSAT2 .....	7
	3.4 Additional Models .....	9
IV.	SIMULATION OF A HYPOTHETICAL SLOPE .....	11
	4.1 Description of a Hypothetical Hillslope .....	11
	4.2 Simulations .....	13
	4.2.1 MODFLOW Simulations .....	14
	4.2.2 PLASM Simulations .....	20
	4.2.3 UNSAT2 .....	24
V.	DISCUSSION .....	27
VI.	CONCLUSIONS .....	30
VII.	REFERENCES .....	32

### APPENDICES

- A. MODFLOW and PLASM Comparisons
- B. MODFLOW Sample Data Files
- C. PLASM Code and Sample Data Files
- D. Program "SWAP"

### LIST OF FIGURES

Figure 4.1-1	Slope Description -- 100% slope .....	12
Figure 4.2.1-1	Lengthwise cross-section of 100% slope showing variations in water table elevations with varying hydraulic conductivity .....	17
Figure 4.2.1-2	Lengthwise cross-section of 100% slope showing variations in water table elevations with varying specific yield .....	19

### LIST OF TABLES

3.2-1	Spreadsheet-style Data Entry Format for PLASM .....	pocket
4.2.1-1(a)	MODFLOW Simulations .....	15
4.2.1-1(b)	MODFLOW Simulations .....	16
4.2.2-1(a)	PLASM Simulations .....	21
4.2.2-1(b)	PLASM Simulations .....	22

## 1. INTRODUCTION

### 1.1 Purpose of Project

Ground-water flow is known to be an important factor in understanding slope stability on steep slopes. The purpose of this project was to evaluate selected ground-water flow models for use in simulating ground-water flow in shallow aquifers on steep slopes.

### 1.2 Selection of Models for Comparison

Two categories of numerical ground-water flow models are applicable to understanding ground-water flow in the context of slope stability: models that simulate only saturated flow and models that simulate variably-saturated flow. In general, saturated flow models calculate head levels (positive pressure head) based on the saturated hydraulic conductivity of the aquifer, a storage term (specific yield or specific storage, depending on aquifer type), initial head values, and the appropriate boundary conditions. The variably-saturated flow models calculate pressure head (positive or negative pressure) in the flow system, but require additional aquifer data describing the relative conductivity as a function of moisture content, pressure head as a function of moisture content, and porosity.

Three models are reviewed as part of this project. Two models are saturated flow models: MODFLOW, developed by the

U.S.G.S. (McDonald and Harbough, 1984), and PLASM (Prickett and Lonquist, 1971). Both of these models are frequently used for ground-water flow modeling. Both models are applied to a theoretical steep slope; output under a variety of conditions is compared for consistency and numerical stability. The third model reviewed is UNSAT2, a variably-saturated flow model written by Neuman, Feddes, and Bresler (1974). UNSAT2 has some inherent limitations when used for simulating steep slope applications, and requires more extensive subsurface data for reliable results than the saturated flow models. Therefore, UNSAT2 is not used in direct comparisons with the other two saturated flow models. Finally, several additional numerical models are discussed in Section 3.4.

All models considered are available in the public domain. In contrast to many proprietary models, source codes are generally provided allowing the understanding and modification of the model.

## 2. BACKGROUND

A literature search of current ground-water research was conducted using "Ground Water Online", an extensive data base supported and maintained by the National Water Well Association. Very few citations were reported concerning ground-water flow modeling on steep slopes. Research has been conducted on ground-water flow in steep bluffs along

the shores of Lake Michigan (Sterret and Edil, 1982), where bluff erosion is of major concern. Water table fluctuations in two aquifers above the toe of a bluff were found to have significant influence on the stabilities of the bluff.

Iverson and Major (1986) analyzed seepage vectors in a cohesionless soil mass subject to steady, uniform, Darcian seepage; a general analytical solution for the limiting stable slope angle in the cohesionless soil mass was derived.

No applications of standard numerical ground-water flow models to steep slope sites were reported in this data base.

### 3. DESCRIPTION OF MODELS

#### 3.1 MODFLOW

MODFLOW is a block-centered, three-dimensional ground-water flow model developed and supported by the U.S. Geological Survey. Based on previous U.S.G.S. flow models developed by Trescott (1975) and Trescott, Pinder, and Larson (1976), MODFLOW uses a modular programming structure with computational and hydrologic functions grouped together in such a way that each function is independent of other functions. The model has been used by the U.S.G.S. and others for the computer simulation of ground-water flow.

The model solves the three-dimensional ground water flow equation, and can be used for either two- or three-

dimensional applications. Multiple layers can be simulated as either confined or unconfined aquifers, or as a combination of confined or unconfined. The model can simulate the effects of a variety of external stresses, such as wells, recharge, rivers, drains, evapotranspiration, and general head boundaries. Two solution algorithms are included in the model: the Strongly Implicit Solution (SIP), and the Slice Successive Overrelaxation method (SSOR).

The model has been designed to run on a variety of different computers. For this project a version modified for use on microcomputers by the International Ground Water Modeling Center (IGWMC) was used (sample data files are provided in Appendix B).

A preprocessor (also distributed by the IGWMC) was used to construct individual data files. The preprocessor is an interactive program that prompts for the appropriate parameters and characteristics, and creates a data file for use with the main program. Because the MODFLOW code is written in a modular format, a different data file is required for each module invoked. The preprocessor automatically generates all of the necessary files.

Data required for the simulations in this report include:

- definition of boundary nodes
- initial head values
- length of stress periods
- number of stress periods
- time step multiplier

- anisotropy ratios
- cell lengths and widths
- storativity/specific yield
- hydraulic conductivity along rows and columns
- bottom elevation of the aquifer
- vertical hydraulic conductivity (for multiple layers)
- recharge rates

Any consistent set of length and time units may be used with MODFLOW.

Several output options are available, including printouts of head values, drawdowns, and cell-by-cell flow terms at each time step. Head values also can be sent to disk for subsequent graphics plots.

### 3.2 PLASM

The Prickett-Lonnquist Aquifer Simulation Model (PLASM -- Prickett and Lonnquist, 1971) is one of the older numerical ground-water flow models in use today. The model was selected for this project because of its history of use, its relative simplicity, and its relative ease of modification.

Also written in FORTRAN, the model consists of a basic node-centered, finite difference simulation program. The mathematical background is well described in the documentation. Various possible modifications are listed in the documentation for incorporating special options such as variable pumping rates, leaky artesian conditions, induced infiltration, ground-water evapotranspiration, water table



conditions, and multiple layers. Because the model is relatively simple, additional modifications are easy to make.

The code used for this project (Appendix C) was modified to simplify data entry and printout options. The dimension statements in the code can be modified to accommodate larger grids. Written in FORTRAN, the model can be run on a variety of computers supporting a FORTRAN compiler.

Data required for basic simulations under water table conditions include:

- number of time steps (days);
- initial time step size (days);
- error criteria for closure (further discussed in Section 4.2.2);
- number of columns;
- number of rows;
- time step multiplier;
- nodal spacing in the x and y directions;
- transmissivity (gal/ft/day) in the x and y directions;
- initial head values;
- pumping/recharge rates (gal/day);
- specific yield;
- permeability in the x and y directions (gal/day/ft<sup>2</sup>); and
- bottom elevation of the aquifer.

Aquifer parameters can be specified differently at all nodes, allowing simulation of anisotropic and heterogeneous conditions. A non-uniform grid also can be specified. Boundaries are specified by manipulating the storage or transmissivity/permeability values at boundary nodes, e.g., a storage term of  $1 \times 10^{-10}$  will create a node with virtually

unlimited storage (constant head); no-flow nodes are created by setting the transmissivity/permeability equal to zero.

Data entry consists of two files: a default file and a specific value file. All nodes not described by specific values in the latter file are defined by default values. Sample data files and format are given in Appendix C.

All nodal characteristics must be listed for any node having an input value different from the default value. On a steep slope this may include all nodes, because most all nodes are simulated with varying initial heads and bottom elevations. To allow easy modification of values for sensitivity runs a Lotus 123 (tm) spreadsheet was used to create the specific value file. As shown in Table 3.2-1 (in pocket), all parameters are listed in matrix form corresponding with respective grid locations. The values are referenced automatically to the right of the data matrices using the spreadsheet's referencing capabilities. Specific value files then consist of the nodal values on the right. This method allows easy visualization and modification of input parameters for the model.

### 3.3 UNSAT2

UNSAT2 is a numerical saturated-unsaturated ground-water flow model developed by Neuman, Feddes, and Bresler (1974). The model can accommodate non-uniform flow regions with irregular boundaries and random local anisotropies.

Flow can be modeled in a vertical plane, a horizontal plane, or in three-dimensions with radial symmetry.

The model emphasizes the simulation of atmospheric boundaries, such as seepage faces, evaporation, infiltration surfaces, and water uptake by plant roots. Solution to flow equations are numerically approximated using the Galerkin method/finite element approach. The finite element method allows the description of irregularly shaped boundary conditions.

The governing equations are expressed in terms of a single variable, pressure head. The total head is given by the combination of the pressure head and the vertical distance above a horizontal datum plane. In the saturated zone the pressure head is positive, whereas the pressure head reaches negative values in the unsaturated zone.

UNSAT2 was written in FORTRAN IV, and can be used on a variety of computers. The program has been modified such that when instabilities occur in the program it returns to the last completed time step, the time step is reduced by one half, and solution process continues (Bloomsburg, 1983).

The hydraulic properties required for each porous material being simulated in the model include:

- saturated conductivity;
- relative conductivity as a function of moisture content;
- porosity;
- pressure head as a function of moisture content;
- specific storage; and
- initial values of pressure head.

Once the hydraulic properties have been identified, a finite element mesh can be superimposed on the flow system.

Sample data files are provided in the documentation for the model. The data file is constructed using a standard editing or word processing program.

### 3.4 Additional Models

Several other models are available which may have application to modeling ground-water flow on steep slopes. Much of the following information was obtained through personal communication with staff at the International Ground Water Modeling Center (IGWMC), Indianapolis, Indiana.

SUTRA (Saturated-Unsaturated Transport), is a variably-saturated flow and solute transport model available for mainframe computers. The model contains analytical functions describing moisture content, pressure head, and relative conductivity relationships which may need to be modified (in the code) for use with other applications.

FEMWATER and FEMWASTE (developed by George Fey, Oak Ridge National Laboratory) are two finite element programs for modeling flow and solute transport in variably-saturated conditions. Previous versions have been described as cumbersome, although the model has recently received some updating. A three-dimensional version may be available for use with microcomputers soon.

Another variably-saturated flow code has recently been developed by the U.S.G.S (Lappala, Healy, and Weakes, 1987). VS2D (Variably-Saturated, two-dimensional) is a finite difference code for simulating two-dimensional movement of water in variably-saturated porous media. Non-linear boundary conditions treated by the code include infiltration, evaporation, and seepage faces. The authors suggest that the finite difference method has several advantages over the finite element method, including: (1) the capability of better handling non-linear phenomena such as infiltration into dry soils and discontinuities in permeability and/or porosity; (2) less numerical manipulation required solving non-linear equations; and (3) less required computer core storage and solution time.

In summary, the two saturated flow models compared in this project were chosen for their relative ease of use, their adaptability to various applications, good documentation and support, and availability in the public domain. In concept, variably-saturated flow models offer several advantages over saturated-only flow models, but additional data requirements and greater complexity create greater limitations to their use.

#### 4. SIMULATION OF A HYPOTHETICAL SLOPE

##### 4.1 Description of a Hypothetical Hillslope

A hypothetical hillslope was used to simulate groundwater flow on steep slopes for the comparison of the two saturated flow models. The first simulations are of a horizontal area measuring 200 feet by 100 feet was assumed (Figure 4.1-1) , with a saturated zone measuring 20 feet in vertical thickness, beginning at 20 vertical feet below grade surface. The bottom of the aquifer, located at 40 vertical feet below grade, is assumed to be impermeable bedrock. The upper and lower boundaries of the site are defined as constant head boundaries -- reflecting, for instance, a slope with the upper boundary being a ridge top and the lower boundary being an imaginary creek. The slope of the hillslope was initially assumed to be 100%, with a total fall over the 200 feet length of 200 feet.

The aquifer materials were assumed to consist of fine- to coarse-grained sands, typical of granitic soils in North-Central Idaho. Saturated hydraulic conductivity was assumed to range from 0.05 feet/day to 50 feet per day, the specific yield of the unconfined aquifer was considered to be in the range of 0.05 to 0.30. (Estimates of hydraulic conductivity reported for one steep slope in the Dan Lee Ridge area of the Clearwater National Forest in Idaho were reported to range from 0.00152 to 0.0134 cm/sec, or 4.31 to 37.98 ft/day -- Woessner, 1968.) Recharge was added to the

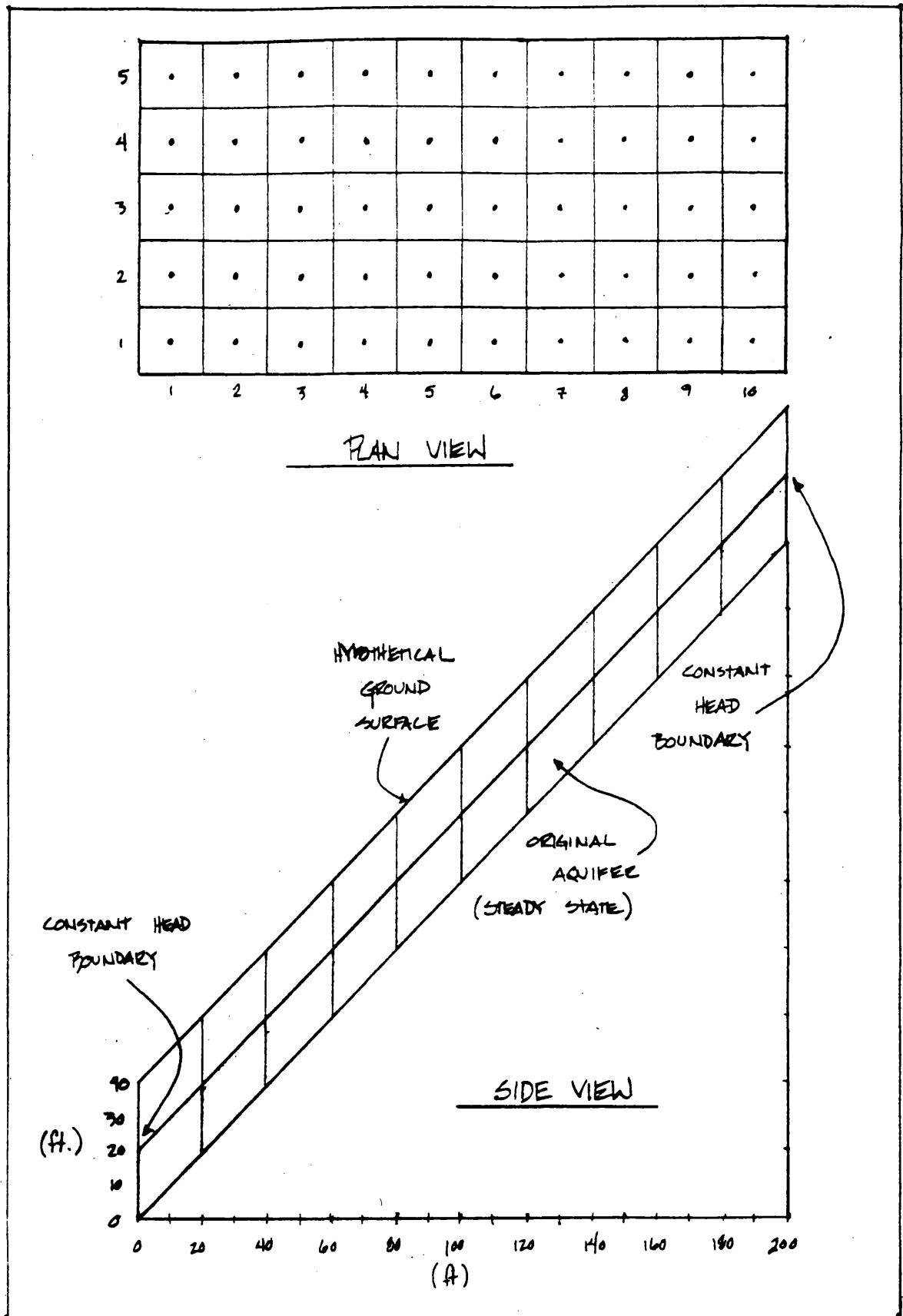


Figure 4.1-1 Description of Hypothetical Slope

hypothetical system at an assumed maximum rate of 0.134 ft/day for 30 days, corresponding to a maximum infiltration rate of 48 inches per month.

A 200% slope was also simulated. A 200% slope with a 20 foot thick aquifer consisting of unconsolidated materials is not a realistic field condition, but was simulated here to test the flow models under extreme conditions. In this case, the horizontal area of each node was redefined as 10 feet by 10 feet, instead of the 20 by 20 foot node size considered above. The initial head values remained the same, giving an overall horizontal slope dimension of 100 by 50 feet, with 200 feet of vertical fall along the length of the slope. Finally, several simulations were conducted of a theoretical five-foot thick aquifer, to test for possible numerical instabilities under mathematically extreme conditions.

Model sensitivity was evaluated for a variety of parameters under different flow conditions, beginning with a range of hydraulic conductivity and storage values but also including the number of time steps (discretization of time), x-y nodal spacing (discretization of space), number of iterations, tolerance limit required for convergence, and recharge patterns. Results of these saturated flow simulations are discussed in the next section.



## 4.2 Simulations

Simulations of hypothetical slopes using the two saturated ground-water flow models are described in this section. The purpose of the simulations is to compare model output generated by the models for consistency, and to test for possible numerical instabilities that may occur in the models when applied to a steep slope. UNSAT2 is not considered here due to the different input data and format required, and to limitations of the variably-saturated flow model itself for steep slope applications.

### 4.2.1 MODFLOW Simulations

Simulations conducted with MODFLOW are shown in Tables 4.2.1-1(a) and 4.2.1-1(b). Two slope angles were modeled -- 100% and 200% slopes -- by varying the x and y dimensions of each model between 10 and 20 feet, leaving initial head values at the upper and lower boundaries constant. In addition, a 20 x 5 node model was also simulated. The total horizontal grid size of any simulation is obtained by multiplying the delta x value by the number of columns and the delta y value by the number of rows.

Hydraulic conductivity was simulated over a range of 0.05 to 50 feet per day, which was thought to represent a reasonable range for sandy, granitic soils. Figure 4.2.1-1 illustrates head levels on the 100% slope after a period of 30 days with a recharge rate of 0.134 feet of infiltration

## MODFLOW SIMULATIONS

Run	Number Rows	Number Cols.	Total Time (days)	Number Time Periods	Number Time Steps/ Period	Del X (ft)	Del Y (ft)	Primary Storage	Hydr Cond (ft/day)	Max Number Iter	Error (feet)	Recharge (ft/day)	Comments
M10	10	5	30	1	10	10	10	0.15	0.50	50	0.01	0.134	Figure 4.2.1-1
M11	10	5	30	1	10	10	10	0.15	0.05	50	0.01	0.134	Figure 4.2.1-1
M12	10	5	30	1	10	10	10	0.15	50.00	50	0.01	0.134	Figure 4.2.1-1
M13	10	5	30	1	10	20	20	0.15	0.50	50	0.01	0.134	Figure 4.2.1-2
M14	10	5	30	1	10	20	20	0.05	0.50	50	0.01	0.134	Figure 4.2.1-2
M15	10	5	30	1	10	20	20	0.30	0.50	50	0.01	0.134	Figure 4.2.1-2
M3	20	5	30	1	12	20	20	0.15	0.5	50	0.01	0.134	
M4	20	5	30	1	12	20	20	0.15	0.05	50	0.01	0.134	
M5	20	5	30	1	12	20	20	0.15	50	50	0.01	0.134	
M2J	10	5	90	3	1: 5 2: 20 3: 20	20	20	0.15	0.5	50	0.01	13.4	600' head differences; no collapse in model
M2I	10	5	90	3	1: 5 2: 20 3: 20	20	20	0.15	0.5	50	0.01	0.134	
M2K	10	5	90	3	1: 5 2: 5 3: 5	20	20	0.15	0.5	50	0.01	0.134	very similar to M2I
M2L	10	5	150	3	1: 5 2: 10 3: 10	20	20	0.15	0.5	50	0.01	0.134	
M2M	20	5	150	3	1: 5 2: 10 3: 10	20	20	0.15	0.5	50	0.01	0.134	
M2N	20	5	150	3	1: 5 2: 10 3: 10	10	10	0.15	0.5	50	0.01	0.134	failed to converge in time step 5, time period 1
M2P	20	5	150	3	1: 5 2: 10 3: 10	10	10	0.15	0.5	50	0.1	0.134	failed to converge, time step 9, time period 3

Table 4.2.1-1(a) MODFLOW Simulations

## MODFLOW SIMULATIONS

Run	Number Rows	Number Cols.	Total Time (days)	Number Time Periods	Number Time Steps/ Period	Del X (ft)	Del Y (ft)	Primary Storage	Hydr Cond (ft/day)	Max Number Iter	Error (feet)	Recharge (ft/day)	Comments
M2B	20	5	150	3	1: 5 2: 10 3: 10	10	10	0.15	0.5	100	0.1	0.134	failed to converge, time step 9, time period 3
M2T	20	5	150	3	1: 5 2: 10 3: 10	10	10	0.15	0.5	100	0.5	0.134	
M20	20	5		1	20	2.5	2.5	0.15	0.5	50	0.05	0.134	200% slope; 5 ft aquifer thickness

\* Aquifer thickness in all runs except M20 is 20 feet; aquifer thickness in Run M20 is 5 feet.

Table 4.2.1-1(b) MODFLOW Simulations

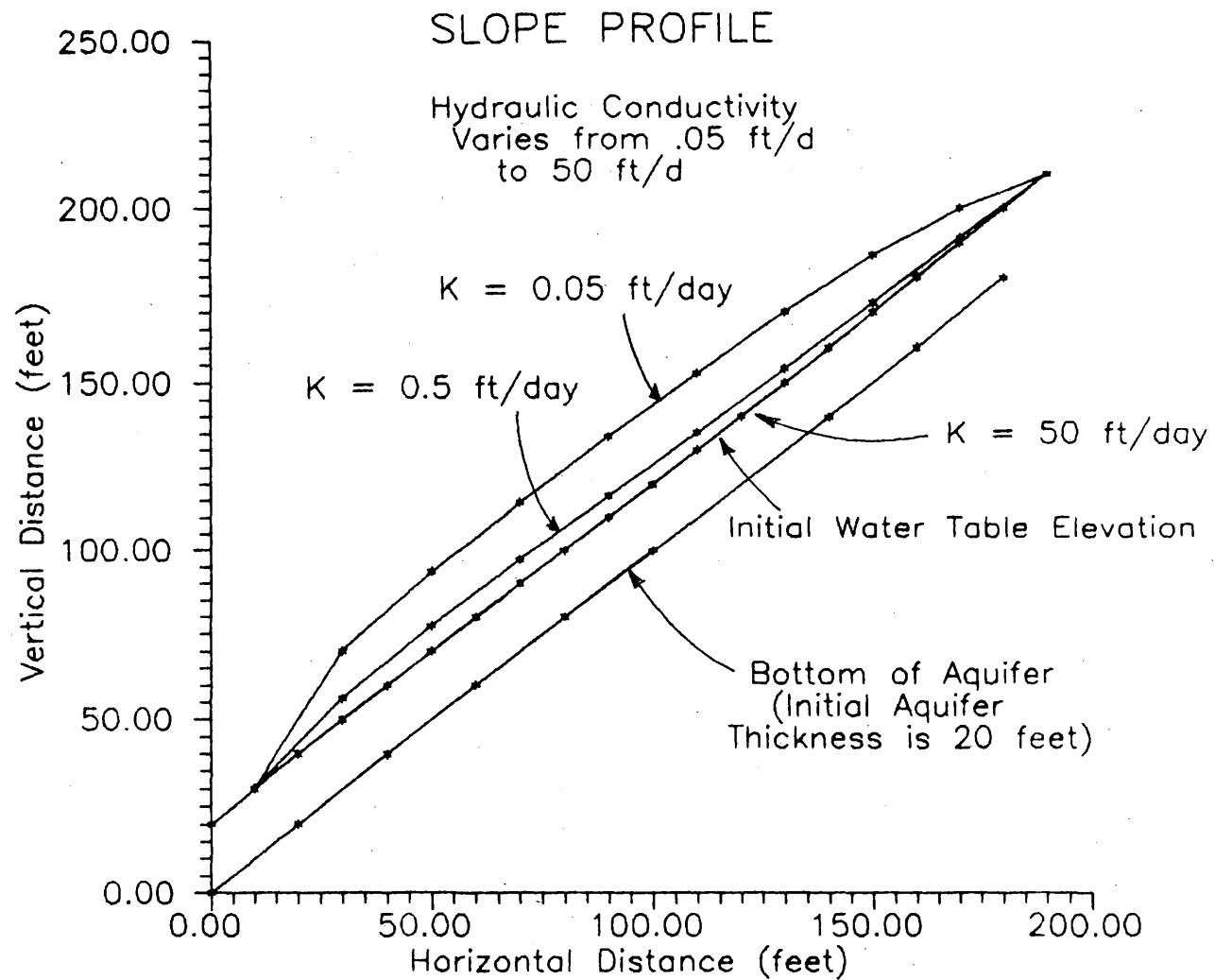


Figure 4.2.1-1 Lengthwise slope profile showing variations in head levels after 30 days due to varying hydraulic conductivity.

per day. Initial head levels and bottom elevations are shown by the straight diagonal lines; head levels for the simulation with a hydraulic conductivity value of 50 feet/day were virtually the same as initial levels. Similarly, specific yield was varied between 0.05 and 0.30. Again, the simulations showed an expected response: the water table rose the highest with the lowest storage value (Figure 4.2.1-2).

To test if unreasonably high infiltration rates would create numerical instabilities in the model, an infiltration rate of 13.4 feet per day (per unit area) for a period of 30 days was simulated on the 100% slope; although head levels rose to over 600 feet in the model (which grossly exceeded the ground surface) no numerical instabilities were evident.

The simulations described above were conducted over a period of 30 days with constant infiltration. A number of runs (M2J - M2T) were conducted over a period of 90 days, divided into three time periods. The first time period lasted for 30 days, with no infiltration occurring. The second time period assumed an infiltration rate of .134 feet/day, and the final 30 day time period again assumed no infiltration. In this configuration, the number of time steps was varied between 5 and 20 per time period, with no significant difference in estimated head values.

Beginning with simulation M2M, the length of the slope was doubled to 400 feet (with a 100 foot width).

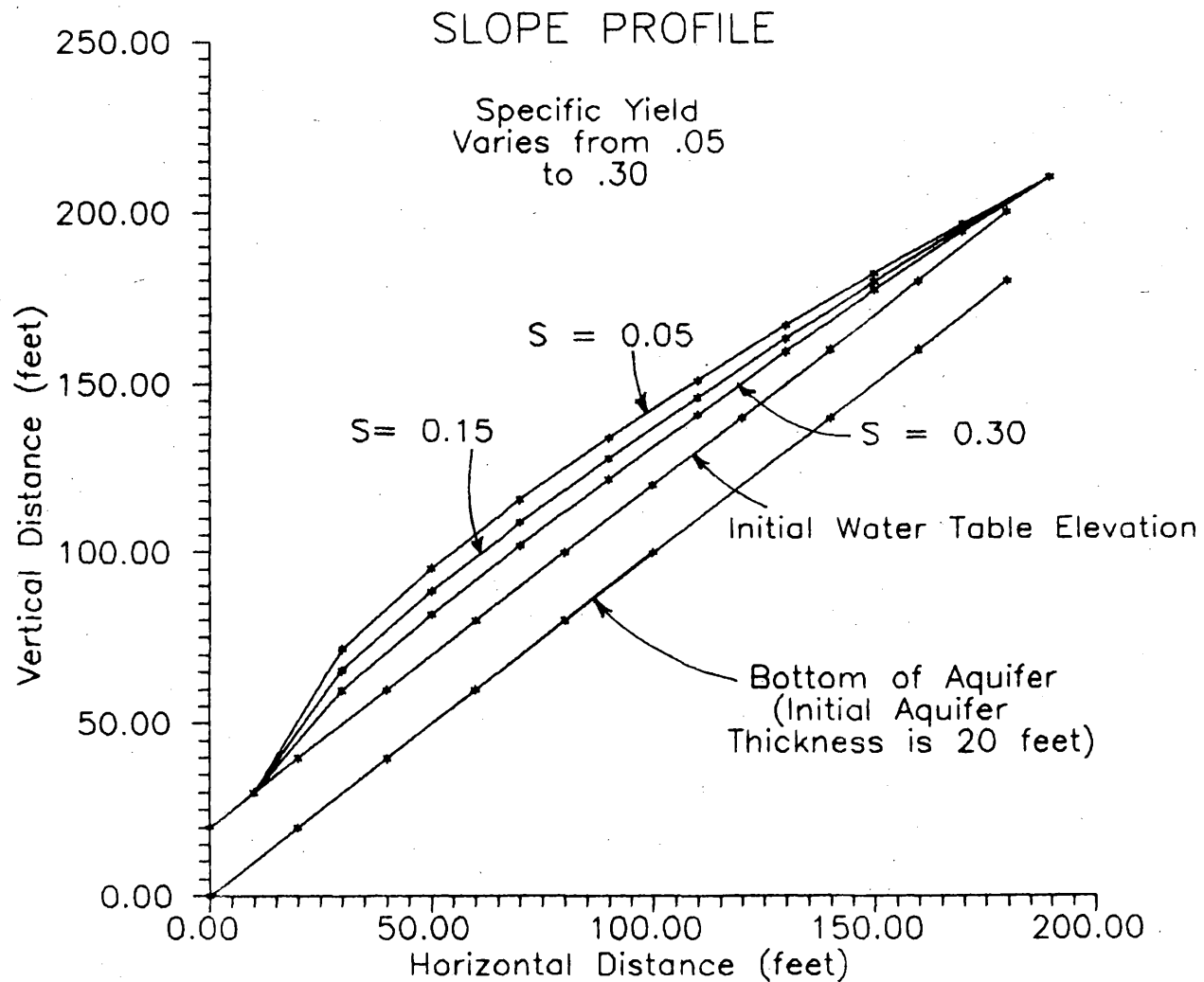


Figure 4.2.1-2 Lengthwise slope profile showing variations in head levels after 30 days due to varying specific yield values.

Instabilities began to occur when the slope of this extended model was changed from 100% to 200% in Run M2N, where the model failed to converge. This could possibly be attributed to the constriction of flow out of the model with a relatively low hydraulic conductivity, such that differences in head at the downgradient slopes became too large between nodes. Increasing the allowable tolerance (the maximum change in head at any one node between iterations) for convergence enabled the model to successfully complete the simulation. Theoretically, increasing the number nodes covering a given area, and/or reducing the time step size and multiplier would allow simulation of these steep conditions by decreasing the discretization of time and space. Although the number of iterations were doubled in Run M2Q without successful simulation completion, increasing the number of iterations even further may also allow successful simulation of a steep slope. Finally, a five-foot thick aquifer on a 200% slope was simulated (Run M2O). No significant numerical instabilities were encountered in this run.

#### 4.2.2 PLASM Simulations

Similar simulations were conducted with the PLASM model as with the MODFLOW code. PLASM simulations are shown in Tables 4.2.2-1(a) and 4.2.2-1(b).

## PLASM SIMULATIONS

Run	Number			Time Step Multiplier	Del X (ft)	Del Y (ft)	Primary Storage	Hydr Cond (ft/day) (g/ft2/d)	Error (feet)	Recharge (ft/day) (g/d/node)	Comparable		Comments
	Total Time (days)	Steps/ Period	Delta (days)								MODL	FLOW	
P25	30	11	0.933	1.2	10	10	0.15	0.50 3.74	0.7	0.134			
P26	30	11	0.933	1.2	20	20	0.15	0.50 3.74	0.7	0.134	M3		
P30	30	11	0.933	1.2	10	10	0.15	0.50 3.74	0.7	0.134	M10		
P31	30	11	0.933	1.2	10	10	0.15	0.05 0.37	0.7	0.134	M11		
P32	30	11	0.933	1.2	10	10	0.15	50.00 373.97	0.7	0.134	M12		
P33	30	11	0.933	1.2	20	20	0.15	0.50 3.74	0.7	0.134	M13		
P34	30	11	0.933	1.2	20	20	0.05	0.50 3.74	0.7	0.134	M14		
P35	30	11	0.933	1.2	20	20	0.30	0.50 3.74	0.7	0.134	M15		
P13	60	15	0.733	1.2	10	10	0.15	0.50 3.74	0.7	0.134	M2L		
P12	30	11	0.933	1.2	20	20	0.15	0.50 3.74	0.7	13.4	M2J		
P7	30	11	0.933	1.2	20	20	0.15	0.05 0.37	0.7	0.134	M4		
P8	30	11	0.933	1.2	20	20	0.15	50.00 373.97	0.7	0.134	M5		
P42		30	0.933	1	10	10	0.15	0.5 3.74	10	0.134		Failed to converge @ 12.13 days	
P43		100	0.2	1	10	10	0.15	0.5 3.74	10	0.134		failed to converge @ 11.8 days	

Table 4.2.2-1(a) PLASM Simulations



## PLASM SIMULATIONS

Run	Number		Time Step	Delta Multiplier	Del X (ft)	Del Y (ft)	Primary Storage (g/ft <sup>2</sup> /d)	Hydr Cond		Error (feet)	Recharge Comparable		Comments
	Total Time (days)	Steps/ Period						(ft/day)			(ft/day)	MODFLOW Run	
P49*	30	0.01	1		2.5	2.5	0.15	0.5	1	0.134			failed to converge @ .1 days
								3.74					
P50*	30	0.01	1		2.5	2.5	0.15	0.5	10	0.134			simulation completed
								3.74					
P51*	300	0.1	1		2.5	2.5	0.15	0.5	10	0.134			N20 simulation completed
								3.74					

\* These simulations were conducted using a 20 x 5 grid with an overall elevation change of 100 feet along the length of the slope, i.e., a 200% slope. All other runs were based on a 10x5 grid.

Table 4.2.2-1(b) PLASM Simulations (cont)

Eight PLASM and MODFLOW slope simulations are compared in Appendix A. The differences between the simulations are negligible; the greatest difference is seen between Runs M2L and P13, with an average difference of 3%.

During simulations preliminary to the runs shown in Table 4.2.2-1, it was found that no simulations on the 100% slope would complete solution with an error value of less than 0.7 feet. In contrast with the specified tolerance value between iterations in MODFLOW, the error in PLASM is a cumulative value representing the total maximum cumulative head change allowable before successfully completing a time step. Thus, an error of 0.7 feet represents an average error of 0.01 feet per node for a 50 node grid (10 x 5), which represents a comparable level of accuracy to the MODFLOW model.

Several simulations were conducted of a hypothetical five-foot thick aquifer at a slope of 200% (Runs P42-P51). It was found that successful convergence required a greater error allowance than previous runs, finer mesh (greater discretization of space), and/or smaller time steps and smaller time step multipliers (greater discretization of time). Despite the unlikely slope conditions, the model was able to successfully complete the simulations with the above adjustments. Simulated head values after 30 days between the MODFLOW and PLASM runs compared very well (Runs M20, P51, Appendix A).

#### 4.2.3 UNSAT2

No actual simulations of the theoretical slope were conducted with the UNSAT2 model, due to the additional data requirements of the model and limitations in using the model on actual steep slopes. These limitations and additional data requirements are discussed in the following paragraphs.

The UNSAT2 variably-saturated flow model can be used to simulate two-dimensional flow in either a horizontal or vertical plane. However, in a horizontal plane it is not possible to specify a bottom aquifer elevation. Thus on a steep slope the bottom of the aquifer would be constant at the elevation of the lowest point of the slope. This limits the model in its present form for use on steep slopes in a two dimensional vertical plane only.

Additional data describing a steep slope aquifer is required before UNSAT2 can be used. As listed in Section 3.4, relative conductivity and pressure head as a function of moisture content is required, as well as porosity data. These additional data requirements may provide obstacles to the use of UNSAT2 on steep forested slopes where few subsurface data exist.

Developing data files for use with UNSAT2 is more difficult than for the two previous models. While a finite element mesh can more accurately portray a randomly-shaped flow systems, mesh development can be a more tedious process

than with a finite difference model. Each triangle or quadrilateral in the mesh must be specified with its coordinate points. A change in slope would require a complete redefinition of the mesh. A preprocessing routine that would define the mesh would be very helpful in facilitating use of this program.

Despite the model's limitations (more extensive data required, limited to vertical two-dimensional applications on steep slopes), the model offers several advantages over the finite difference saturated flow models. UNSAT2 is capable of simulating seepage faces, which may play a significant role in flow systems on steep slopes. Furthermore, the model has extensive capabilities of simulating the effects of vegetation and infiltration. Input options include: the number of evaporation and infiltration boundary nodes, number of plant species, number of vertical columns in root zone for any plant species, maximum allowed rate of evaporation or infiltration normal to soil surface, wilting pressures of various plant species, maximum transpiration rates of various plant species, and root effectiveness functions. The program will also simulate seepage faces within a well completed in an unconfined aquifer.

One author proposes a methodology for quasi three-dimensional application of UNSAT2 to first order watersheds (DeGroot, 1987). Termed the method of "sectional

partitioning", the horizontal planar surface area of a first order watershed is divided into convergent, divergent, and parallel sections, each section a sub-area of the watershed. Viewed from the side, the sub-areas would appear as vertical cross-sections, with either variable or constant width. Each section is thus rendered into a two dimensional vertical or axisymmetric subsurface flow simulation problem (Figure 1-3 and 1-4 in DeGroot, 1987) and the flow system of the entire watershed is represented by the integrated response of each partitioned section.

DeGroot suggests that data describing the watershed should include: boundary conditions and elevations, precipitation distribution, snowpack water depth, snow melt rates and losses to sublimation and evaporation, porosity and hydraulic conductivity of all porous media in the flow system, unsaturated porous media characteristics (as described earlier), streamflow records at the outlet of the watershed, and evaporation and transpiration data.

DeGroot cautions that the watershed should not be partitioned so that one section flows into another, since boundary flux calculations are difficult to determine. For instance, if two convergent sections (axisymmetric) were linked together, the flux at the inner radius of one section would not equal the flux at the outer radius of the other.

## 5. DISCUSSION

A variety of saturated- and variably-saturated numerical ground-water flow models are available for application to steep slope flow systems. Three models were considered in detail during the course of this project.

Based on preliminary simulations with two saturated flow models (MODFLOW and PLASM) of a theoretical steep slope flow system, it appears that both models give predictable and consistent results. As slopes increase, the models require increasingly finer grids and smaller time steps for successful simulation. Very little discrepancy is found in comparing selected simulations (Appendix A). Further validation of the use of these models for steep slope flow systems could be done based on actual field data.

The saturated flow models discussed in this report have several advantages over the variably-saturated flow model (UNSAT2) for use with steep slope applications. Both models are relatively easy to use, with MODFLOW having the additional advantage of a preprocessing program for the preparation of data files (although it was found that a standard spreadsheet program could also be used to easily develop and modify data files for the PLASM model). MODFLOW also comes with a postprocessing program which allows transforming a rectangular map of potentiometric head elevations into x-y-z data format for use with popular two- and three-dimensional plotting programs.

(To facilitate the use of these and other models a FORTRAN program is included with this report (program "SWAP", Appendix D) which transforms rectangular matrix-form head data from an output file into x-y-z plotting data. In addition, axis origins are transformed consistent with the flow model and plotting routine requirements.)

Both saturated flow models considered in this report are well documented, are relatively easy to understand and modify for specialized uses.

MODFLOW is written and validated to simulate a multi-layer flow system with varying hydraulic properties -- the model numerically solves the three-dimensional flow equation (McDonald and Harbough, 1984). PLASM can be modified to simulate some forms of three-dimensional flow -- in this case the model would separately simulate "leakance" from layers above and below into a given cell.

These models are limited to the simulation of saturated flow only. On steep slopes with sandy soils, with a relatively small tension-saturated zone (i.e., the capillary pressure-saturation curve approximates a step function) this may not be a significant limiting factor. Furthermore, the saturated flow models are unable (without modification) to simulate the development of seepage faces due to the rising water levels of shallow aquifers. Finally, boundary portrayal is limited to finite difference grid constraints (although this would not be true of finite element models).

UNSAT2 offers several advantages over the saturated flow models, but its use also has limitations. First, UNSAT2 can simulate the effects of seepage faces and general unsaturated flow. However, on steep slopes where the change in the bottom elevation of an aquifer over the length of the aquifer is significant the model can only be used in two-dimensional vertical (or axisymmetric) applications. Utilizing the advantages of UNSAT2 requires additional data about the flow system, as discussed in Section 3.3. If limited data are available for a site and the flow analysis is being used for hypothetical scenario evaluation, the variably-saturated flow model is at a disadvantage because of its additional data requirements.

DeGroot (1987) presents a method for using UNSAT2 for modeling flow in a first order watershed, in a quasi three-dimensional sense. However, the basin model consists of partitions limited by the same constraints mentioned above; it does not appear that the method would enhance simulation of just one slope in a watershed.

Several other variably-saturated flow models were briefly discussed in Section 3.4. Of these, a variably-saturated flow model which holds promise is the VS2D model being developed by the U.S.G.S., although this model is limited by some of the same constraints as is UNSAT2.

In summary, if saturated flow is the major concern in modeling steep slope aquifers, both of the saturated-flow



models appear to be suitable. If variably-saturated flow is of primary concern, UNSAT2 or VS2D may be adequate, given their limitations. Additional testing of these models could be conducted once more field data are available.

Calibrating a model(s) to an actual site would require field data describing seasonal head elevations (the number of points would depend on the topographical irregularity of the site, understanding of boundary conditions, heterogeneity and anisotropy of the aquifer, etc.), hydraulic characteristics of the aquifer, bottom elevation of the aquifer, and an understanding of boundary conditions. Additional verification of a model would rely on data describing the aquifer response to stimulus, e.g., pumping or a precipitation event.

## 6. CONCLUSIONS

Of several saturated- and variably-saturated groundwater flow models considered during the course of this project, three models were examined in detail: MODFLOW, PLASM, and UNSAT2. Preliminary simulations of two-dimensional horizontal flow systems (although both models can be used to simulate three-dimensional flow) suggest that both MODFLOW and PLASM can be used for simulating thin, shallow aquifers on slopes as high as 100% to 200%. As slopes become steeper an increasingly finer grid and smaller time steps are required for satisfactory model simulation.

Both of these saturated-flow models gave predictable and consistent results for the simulations conducted.

UNSAT2, as a variably-saturated flow model, has the advantage of being able to simulate unsaturated flow conditions. However, significantly more input data are required than for the saturated-flow models -- data that may often be unavailable for typical field situations. In addition, the model in its present form is limited to use in two dimensions, and for a steep slopes can only be used in the vertical plane.

## 7. REFERENCES

- Bloomsburg, G.L., and R.E. Rinker, Ground water modeling with an interactive computer, *Ground Water*, 21(2), 1983.
- DeGroot, Philip H., Simulation of Variably Saturated Subsurface Flow by Sectional Partitioning, Ph.D. Dissertation, Utah State University, Logan Utah, 1987.
- Iverson, Richard M., and Jon J. Major, Ground water seepage vectors and the potential for hillslope failure and debris flow mobilization, *Water Resources Research*, 22(11), 1543-1548, 1986.
- Lappala, E.G., R.W. Healy, and E.P. Weeks, Documentation of Computer Program VS2D to Solve the Equations of Fluid Flow in Variably Saturated Porous Media, U.S. Geological Survey, Water-Resources Investigations Report 83-4099, 1987.
- McDonald, Michael G., and Arlen W. Harbough, A Modular Three-Dimensional Finite Difference Ground Water Model, U.S. Geological Survey, Ground Water Branch, Reston, Virginia, 1984 (available from Scientific Publications, P.O. Box 23041, Washington D.C., 20026-3041).
- Neuman, Shlomo P., Reinder A. Feddes, and Eshel Bresler, Finite Element Simulation of Flow in Saturated-Unsaturated Soils Considering Water Uptake by Plants, "Development of Methods, Tools, and Solutions for Unsaturated Flow", Third Annual Report (Part 1), Project No. ALO-SWC-77, Grant No. FG-Is-287, U.S.D.A., Haifa Israel, July, 1974.
- Prickett, T.A., and C.G. Lonquist, Selected Digital Computer Techniques and Groundwater Resource Evaluation, Illinois State Water Survey, 1971.
- Sterret, Robert J., and Tuncer B. Edil, Ground water flow systems and stability of a slope, *Ground Water*, 20(1), 5-11, 1982.
- Woessner, William W., Final Report -- Cooperative Agreement: Intermountain Research Station, USDA-FS, and the Geology Department, University of Montana, Prepared for Rod Prellwitz, Intermountain Research Station, Missoula, Montana, by the author at the Department of Geology, University of Montana, Missoula, 1986.

**APPENDIX A**  
**MODFLOW AND PLASM COMPARISONS**

MODFLOW - PLASM COMPARISONS

MODFLOW Run	M3	M2L
PLASM Run	P16,P26	P13
delta X	20	20
Delta Y	20	20
Sy	0.15	0.15
K (ft/d)	0.5	0.5
Recharge (ft/d)	0.134	0.134
Time (d)	30	60

M	P	% Dif	M	P	% Dif
210.00	210.00	0.0000	210.00	210.00	0.0000
195.37	195.50	0.0007	195.16	196.32	0.0059
179.79	180.03	0.0013	179.31	181.85	0.0142
163.34	163.69	0.0021	162.57	166.55	0.0245
146.08	146.51	0.0029	145.04	150.35	0.0366
128.01	128.47	0.0036	126.75	133.08	0.0499
108.98	109.39	0.0038	107.58	114.41	0.0635
88.59	88.79	0.0023	87.19	93.70	0.0747
65.68	65.34	0.0052	64.46	69.41	0.0768
30.00	30.00	0.0000	30.00	30.00	0.0000
Average Difference:		0.0022			0.0346

MODFLOW Run	M10	M11
PLASM Run	P30	P31
delta X	10	10
Delta Y	10	10
Sy	0.15	0.15
K (ft/d)	0.5	0.05
Recharge (ft/d)	0.134	0.134
Time (d)	30	30

M	P	% Dif	M	P	% Dif
210.00	210.00	0.0000	210.00	210.00	0.0000
191.42	191.42	0.0000	200.06	200.37	0.0015
172.81	172.82	0.0001	186.33	186.79	0.0025
154.15	154.18	0.0002	170.30	170.82	0.0031
135.40	135.44	0.0003	152.74	153.25	0.0033
116.48	116.53	0.0004	134.10	134.54	0.0033
97.25	97.30	0.0005	114.49	114.81	0.0028
77.41	77.42	0.0001	93.61	93.67	0.0006
56.20	56.11	0.0016	70.17	69.54	0.0090
30.00	30.00	0.0000	30.00	30.00	0.0000
		0.0003			0.0026

MODFLOW - PLASM COMPARISONS

MODFLOW Run	M12	M13
PLASM Run	P32	P33
delta X	10	20
Delta Y	10	20
Sy	0.15	0.15
K (ft/d)	50	0.5
Recharge (ft/d)	0.134	0.134
Time (d)	30	30

	M	P	% Dif		M	P	% Dif
	210.00	210.00	0.0000		210.00	210	0.0000
	190.01	190.01	0.0000		195.37	195.5	0.0007
	170.03	170.03	0.0000		179.79	180.03	0.0013
	150.04	150.14	0.0007		163.34	163.69	0.0021
	130.15	130.05	0.0008		146.08	146.51	0.0029
	110.07	110.07	0.0000		128.01	128.47	0.0036
	90.08	90.08	0.0000		108.98	109.39	0.0038
	70.08	70.08	0.0000		88.59	88.79	0.0023
	50.07	50.07	0.0000		65.68	65.37	0.0047
	30.00	30.00	0.0000		30.00	30	0.0000
Average Difference:			0.0001				0.0021

MODFLOW Run	M14	M15
PLASM Run	P34	P35
delta X	20	20
Delta Y	20	20
Sy	0.05	0.3
K (ft/d)	0.5	0.5
Recharge (ft/d)	0.134	0.134
Time (d)	30	30

	M	P	% Dif		M	P	% Dif
	210.00	210	0.0000		210.00	210.00	0.0000
	196.46	196.54	0.0004		194.31	194.42	0.0006
	182.18	182.31	0.0007		177.39	177.61	0.0012
	167.11	167.27	0.0010		159.52	159.81	0.0018
	151.15	151.29	0.0009		140.92	141.24	0.0023
	134.13	134.18	0.0004		121.77	122.09	0.0026
	115.73	115.57	0.0014		102.12	102.41	0.0028
	95.38	94.82	0.0059		81.77	81.97	0.0024
	71.76	70.33	0.0199		59.84	59.80	0.0007
	30.00	30	0.0000		30.00	30.00	0.0000
			0.0031				0.0014

# MODFLOW - PLASM COMPARISONS

MODFLOW Run	M20
PLASM Run	P51
delta X	2.5
Delta Y	2.5
Sy	0.15
K (ft/d)	0.5
Recharge (ft/d)	0.134
Time (d)	30

M	P	% Dif
105.00	105	0.0000
100.40	100.36	0.0004
95.72	95.72	0.0000
91.08	91.08	0.0000
86.44	86.44	0.0000
81.79	81.8	0.0001
77.14	77.16	0.0003
72.49	72.52	0.0004
67.83	67.87	0.0006
63.16	63.22	0.0009
58.48	58.55	0.0012
53.79	53.88	0.0017
49.08	49.18	0.0020
44.34	44.43	0.0020
39.53	39.63	0.0025
34.64	34.73	0.0026
29.6	29.67	0.0024
24.3	24.31	0.0004
18.48	18.37	0.0060
10	10	0.0000
		0.0012

**APPENDIX B**  
**MODFLOW SAMPLE DATA FILES**



type m2.bas

BASIC SLOPE MODEL --- AQUIFER THICKNESS = 5 FEET  
100% AND 200% SLOPE

```
      1      20      5      1      4
      0  0  0  0  0  0 18 19  0  0  0
      0      0
      1      1(40I2)      2
-1-1-1-1-1-1
 1 1 1 1 1
 1 1 1 1 1
 1 1 1 1 1
 1 1 1 1 1
 1 1 1 1 1
 1 1 1 1 1
 1 1 1 1 1
 1 1 1 1 1
 1 1 1 1 1
 1 1 1 1 1
 1 1 1 1 1
 1 1 1 1 1
 1 1 1 1 1
 1 1 1 1 1
 1 1 1 1 1
 1 1 1 1 1
 1 1 1 1 1
 1 1 1 1 1
 1 1 1 1 1
 1 1 1 1 1
 1 1 1 1 1
-1-1-1-1-1-1
999.00
      1      .100E+01(7G11.4)      12
105.0      105.0      105.0      105.0      105.0
100.0      100.0      100.0      100.0      100.0
 95.00      95.00      95.00      95.00      95.00
 90.00      90.00      90.00      90.00      90.00
 85.00      85.00      85.00      85.00      85.00
 80.00      80.00      80.00      80.00      80.00
 75.00      75.00      75.00      75.00      75.00
 70.00      70.00      70.00      70.00      70.00
 65.00      65.00      65.00      65.00      65.00
 60.00      60.00      60.00      60.00      60.00
 55.00      55.00      55.00      55.00      55.00
 50.00      50.00      50.00      50.00      50.00
 45.00      45.00      45.00      45.00      45.00
 40.00      40.00      40.00      40.00      40.00
 35.00      35.00      35.00      35.00      35.00
 30.00      30.00      30.00      30.00      30.00
 25.00      25.00      25.00      25.00      25.00
 20.00      20.00      20.00      20.00      20.00
 15.00      15.00      15.00      15.00      15.00
 10.00      10.00      10.00      10.00      10.00
30.000      201.5000
```

D:\SLOPE\MOD>

type m2.bcf

0 -1

1

0 .100E+01

0 .250E+01

0 .250E+01

0 .150E+00

0 .500E+00

11 .100E+01 (7G11.4)

12

100.0	100.0	100.0	100.0	100.0
95.00	95.00	95.00	95.00	95.00
90.00	90.00	90.00	90.00	90.00
85.00	85.00	85.00	85.00	85.00
80.00	80.00	80.00	80.00	80.00
75.00	75.00	75.00	75.00	75.00
70.00	70.00	70.00	70.00	70.00
65.00	65.00	65.00	65.00	65.00
60.00	60.00	60.00	60.00	60.00
55.00	55.00	55.00	55.00	55.00
50.00	50.00	50.00	50.00	50.00
45.00	45.00	45.00	45.00	45.00
40.00	40.00	40.00	40.00	40.00
35.00	35.00	35.00	35.00	35.00
30.00	30.00	30.00	30.00	30.00
25.00	25.00	25.00	25.00	25.00
20.00	20.00	20.00	20.00	20.00
15.00	15.00	15.00	15.00	15.00
10.00	10.00	10.00	10.00	10.00
5.000	5.000	5.000	5.000	5.000

D:\SLOPE\MOD> type m2.rch

1 0

0 0

0 .134E+00

D:\SLOPE\MOD> type m2.sip

100 5

1.0000 .05000E+00 1.00000 1

D:\SLOPE\MOD>

**APPENDIX C**

**PLASM CODE (LIST FILE)  
SAMPLE DATA FILES**

```

D Line# 1      7      Microsoft FORTRAN77 V3.30 March 1985
1 C BASIC AQUIFIER SIMULATION PROGRAM FOR WATER TABLE CONDITIONS.
2 C -----
3 C DEFINITION OF VARIABLES:
4 C
5 C HO(I,J)-----HEADS AT START OF TIME INCREMENT,AT (I,J)
6 C H(I,J)-----HEADS AT END OF TIME INCREMENT.
7 C SF2(I,J)-----STORAGE FACTOR FOR WATER TABLE CONDITIONS.
8 C Q(I,J)-----CONSTANT WITHDRAWAL RATES.
9 C T(I,J,1)-----AQUIFER TRANSMISSIVITY BETWEEN I,J & I,J+1.
10 C T(I,J,2)-----AQUIFER TRANSMISSIVITY BETWEEN I,J & I+1,J.
11 C NR & NC-----NO.OF ROWS & COLUMNS IN MODEL RESP..
12 C NSTEPS-----NO.OF TIME INCREMENTS.
13 C DELTA-----TIME INCREMENT.
14 C PERM(I,J,1)-AQUIFR PERMEABILITY BETWEEN I,J & I,J+1.
15 C PERM(I,J,2)-AQUIFR PERMEABILITY BETWEEN I,J & I+1,J.
16 C BOT(I,J)-----ELEVATION OF BOTTOM OF AQUIFIER.
17 C TMULT-----MULTIPLYING FACTOR FOR TIME STEP INCREMENT.
18 C NRG-----0 IF GRID IS REGULARLY SPACED, OTHERWISE 1.
19 C MAXIT-----MAXIMUM NUMBER OF ITERATIONS
20 C
21 CHARACTER*64 FN1,FN2,FN3
22 COMMON/FIRST/H(40,40),HO(40,40),SF2(40,40),Q(40,40)
23 COMMON/SECOND/T(40,40,2),DL(40,40),B(40),G(40)
24 COMMON/THIRD/PERM(40,40,2),BOT(40,40),DELX(40),DELY(40)
25 C
26 C** READ THE DEFAULT VALUES *****
27 C
28 WRITE(*,2)
29 2 FORMAT(' Input Default Value File name ? '\)
30 READ(*,1)FN1
31 1 FORMAT(A)
32 OPEN(5,FILE=FN1)
33 WRITE(*,3)
34 3 FORMAT(' Input Specific Value File name ? '\)
35 READ(*,1)FN2
36 OPEN(6,FILE=FN2)
37 WRITE(*,4)
38 4 FORMAT(' Output File name ? '\)
39 READ(*,1)FN3
40 OPEN(7,FILE=FN3,STATUS='NEW')
41 READ(5,*)NSTEPS,DELTA,ERROR,NC,NR,TT,S2,HH,QQ,TMULT,NRG,PP,
42 & BOTT,MAXIT
43 WRITE(*,*)'No. of time steps in simulation: ',NSTEPS
44 WRITE(*,*)'Initial time step size: ',DELTA
45 WRITE(*,*)'Multiplying factor to time step size: ',TMULT
46 WRITE(*,*)'Error criterion chosen for closure: ',ERROR
47 WRITE(*,*)'No. of rows and columns (respectively): ',NR,NC
48 WRITE(*,*)'Default aquifer hydraulic conductivity is: ',PP
49 WRITE(*,*)'Default Storage factor is: ',S2
50 WRITE(*,*)'Default heads are: ',HH
51 WRITE(*,*)'Default bottom elevations are: ',BOTT
52 WRITE(*,*)'Default pumping at each node is: ',QQ
53 WRITE(*,*)'Maximum number of iterations: ',MAXIT
54 C
55 C** FILL ARRAYS WITH DEFAULT VALUES*****
56 C

```

```

D Line# 1      7
57      IF (NRG.EQ.1) THEN
58      READ(5,*) (DELX(I), I=1,NC)
59      READ(5,*) (DELY(I), I=1,NR)
60      ELSE
61      READ(5,*) DEX,DEY
62      DO 20 I=1,NC
1 63 20      DELX(I)=DEX
64      DO 21 J=1,NR
1 65 21      DELY(J)=DEY
66      ENDIF
67      DO 22 I=1,NC
1 68      DO 22 J=1,NR
2 69      T(I,J,1)=TT*DELX(I)*2./(DELY(J)+DELY(J+1))
2 70      T(I,J,2)=TT*DELY(J)*2./(DELX(I)+DELX(I+1))
2 71      SF2(I,J)=S2*DELX(I)*DELY(J)
2 72      H(I,J)=HH
2 73      HO(I,J)=HH
2 74      PERM(I,J,1)=PP*DELX(I)*2./(DELY(J)+DELY(J+1))
2 75      PERM(I,J,2)=PP*DELY(J)*2./(DELX(I)+DELX(I+1))
2 76      BOT(I,J)=BOTT
2 77      DL(I,J)=0.
2 78 22      Q(I,J)=QQ
79 C
80 C**READ NODE CARDS*****
81 C
82 30      READ(6,*,END=50) I,J,T(I,J,1),T(I,J,2),H(I,J),Q(I,J),
83      & SF2(I,J),PERM(I,J,1),PERM(I,J,2),BOT(I,J)
84      T(I,J,1)=T(I,J,1)*DELX(I)*2./(DELY(J)+DELY(J+1))
85      T(I,J,2)=T(I,J,2)*DELY(J)*2./(DELX(I)+DELX(I+1))
86      SF2(I,J)=SF2(I,J)*DELX(I)*DELY(J)
87      HO(I,J)=H(I,J)
88      PERM(I,J,1)=PERM(I,J,1)*DELX(I)*2./(DELY(J)+DELY(J+1))
89      PERM(I,J,2)=PERM(I,J,2)*DELY(J)*2./(DELX(I)+DELX(I+1))
90      GO TO 30
91 C
92 C**START OF SIMULATION*****
93 C
94 50      TIME=0.
95      DO 320 ISTEP=1,NSTEPS
1 96      TIME=TIME+DELTA
1 97 C
1 98 C**PREDICT HEADS FOR NEXT TIME INCREMENT*****
1 99 C
1 100      DO 70 I=1,NC
2 101      DO 70 J=1,NR
3 102      D=H(I,J)-HO(I,J)
3 103      HO(I,J)=H(I,J)
3 104      F=1.
3 105      IF (DL(I,J).EQ.0.0) GO TO 60
3 106      IF (ISTEP.GT.2) F=D/DL(I,J)
3 107      IF (F.GT.5.) F=5.
3 108      IF (F.LT.0.) F=0.
3 109 60      DL(I,J)=D
110 70      H(I,J)=H(I,J)+D*F
111 C
1 112 C**USING THIS FIRST ESTIMATE, USE IADI METHOD*****

```

11-08-88

10:24:58

Microsoft FORTRAN77 V3.30 March 1985

```

D Line# 1      7
1 113 C
1 114      ITER=0
1 115 80      E=0.
1 116      ITER=ITER+1
1 117      IF (ITER.GT.MAXIT) THEN
1 118          WRITE (*,82) ITER,TIME
1 119 82      FORMAT (/// 'Number of Iterations exceeds ',I3,
1 120          & ' at ',F6.2,' days')
1 121          GO TO 340
1 122      ENDIF
1 123 C
1 124 C**TRANSMISSIVITY CONTROL*****
1 125 C
1 126      DO 83 I=1,NC
2 127      DO 83 J=1,NR
3 128          IF (I.LT.NC) THEN
3 129              AVH=ABS((H(I,J)-BOT(I,J))*(H(I+1,J)-BOT(I+1,J)))
3 130              T(I,J,2)=PERM(I,J,2)*SQRT(AVH)
3 131          ENDIF
3 132          IF (J.LT.NR) THEN
3 133              AVH=ABS((H(I,J)-BOT(I,J))*(H(I,J+1)-BOT(I,J+1)))
3 134              T(I,J,1)=PERM(I,J,1)*SQRT(AVH)
3 135          ENDIF
3 136 83      CONTINUE
1 137 C
1 138 C**COLUMN CALCULATIONS*****
1 139 C
1 140      DO 190 II=1,NC
2 141          I=II
2 142          IF (MOD(ISTEP+ITER,2).EQ.1) I=NC-I+1
2 143          DO 170 J=1,NR
3 144 C
3 145 C**CALCULATE B & G ARRAYS*****
3 146 C
3 147          BB=SF2(I,J)/DELTA
3 148          DD=HO(I,J)*SF2(I,J)/DELTA-Q(I,J)
3 149          AA=0.0
3 150          CC=0.0
3 151          IF (J-1) 90,100,90
3 152 90      AA=-T(I,J-1,1)
3 153          BB=BB+T(I,J-1,1)
3 154 100      IF (J-NR) 110,120,110
3 155 110      CC=-T(I,J,1)
3 156          BB=BB+T(I,J,1)
3 157 120      IF (I-1) 130,140,130
3 158 130      BB=BB+T(I-1,J,2)
3 159          DD=DD+H(I-1,J)*T(I-1,J,2)
3 160 140      IF (I-NC) 150,160,150
3 161 150      DD=DD+H(I+1,J)*T(I,J,2)
3 162          BB=BB+T(I,J,2)
3 163 C The program documentation contains an error here.
3 164 160      IF (J-1) 410,420,410
3 165 420      W=BB
3 166          WW=DD
3 167          GO TO 430
3 168 410      W=BB-AA*B(J-1)

```

```

D Line# 1      7
3 169      WW=DD-AA*G(J-1)
3 170 430    B(J)=CC/W
3 171 170    G(J)=WW/W
2 172 C
2 173 C**REESTIMATE HEADS*****
2 174 C
2 175      E=E+ABS(H(I,NR)-G(NR))
2 176      H(I,NR)=G(NR)
2 177      N=NR-1
2 178 180    HA=G(N)-B(N)*H(I,N+1)
2 179      E=E+ABS(HA-H(I,N))
2 180      H(I,N)=HA
2 181      N=N-1
2 182      IF(N.GT.0)GO TO 180
2 183      DO 190 N=1,NR
3 184      IF(H(I,N).GT.BOT(I,N))GO TO 190
3 185      E=E+BOT(I,N)+0.01-H(I,N)
3 186      H(I,N)=BOT(I,N)+0.01
3 187 190    CONTINUE
1 188 C
1 189 C*****TRANSMISSIVITY CONTROL *****
1 190 C
1 191      DO 93 I=1,NC
2 192      DO 93 J=1,NR
3 193      IF(I.LT.NC)THEN
3 194      AVH=ABS((H(I,J)-BOT(I,J))*(H(I+1,J)-BOT(I+1,J)))
3 195      T(I,J,2)=PERM(I,J,2)*SQRT(AVH)
3 196      ENDIF
3 197      IF(J.LT.NR)THEN
3 198      AVH=ABS((H(I,J)-BOT(I,J))*(H(I,J+1)-BOT(I,J+1)))
3 199      T(I,J,1)=PERM(I,J,1)*SQRT(AVH)
3 200      ENDIF
3 201 93      CONTINUE
1 202 C
1 203 C**ROW CALCULATIONS*****
1 204 C
1 205      DO 300 JJ=1,NR
2 206      J=JJ
2 207      IF(MOD(ISTEP+ITER,2).EQ.1)J=NR-J+1
2 208      DO 280 I=1,NC
3 209      BB=SF2(I,J)/DELTA
3 210      DD=HO(I,J)*SF2(I,J)/DELTA-Q(I,J)
3 211      AA=0.
3 212      CC=0.
3 213      IF(J-1)200,210,200
3 214 200      BB=BB+T(I,J-1,1)
3 215      DD=DD+H(I,J-1)*T(I,J-1,1)
3 216 210      IF(J-NR)220,230,220
3 217 220      DD=DD+H(I,J+1)*T(I,J,1)
3 218      BB=BB+T(I,J,1)
3 219 230      IF(I-1)240,250,240
3 220 240      BB=BB+T(I-1,J,2)
3 221      AA=-T(I-1,J,2)
3 222 250      IF(I-NC)260,270,260
3 223 260      CC=-T(I,J,2)
3 224      BB=BB+T(I,J,2)

```

```

D Line# 1      7      Microsoft FORTRAN77 V3.30 March 1985
3 225 C The program documentation contains an error here.
3 226 270 IF(I-1)440,450,440
3 227 450 W=BB
3 228 WW=DD
3 229 GO TO 460
3 230 440 W=BB-AA*B(I-1)
3 231 WW=DD-AA*G(I-1)
3 232 460 B(I)=CC/W
3 233 280 G(I)=WW/W
2 234 C
2 235 C**REESTIMATE HEADS*****
2 236 C
2 237 E=E+ABS(H(NC,J)-G(NC))
2 238 H(NC,J)=G(NC)
2 239 N=NC-1
2 240 290 HA=G(N)-B(N)*H(N+1,J)
2 241 E=E+ABS(H(N,J)-HA)
2 242 H(N,J)=HA
2 243 N=N-1
2 244 IF(N.GT.0)GO TO 290
2 245 DO 300 N=1,NC
3 246 IF(H(I,N).GT.BOT(I,N))GO TO 300
3 247 E=E+BOT(I,N)+0.01-H(I,N)
3 248 300 CONTINUE
1 249 IF(E.GT.ERROR)GO TO 80
1 250 C
1 251 C**PRINT RESULTS*****
1 252 C
1 253 WRITE(7,310)TIME,E,ITER
1 254 310 FORMAT(/,,' TIME=',F6.2,' days',/,,' ERROR=',F7.4,3X,
1 255 & ' ITERATIONS=',I5,/)
1 256 DELTA=DELTA*TMULT
1 257 DO 320 J=1,NR
2 258 320 WRITE(7,330)J,(H(I,J),I=1,NC)
2 259 330 FORMAT(I5,5X,15F8.2/(10X15F8.2))
2 260 WRITE(*,*)'Simulation Complete'
2 261 340 STOP
2 262 END

```

Name	Type	Offset	P	Class
AA	REAL	570		
ABS				INTRINSIC
AVH	REAL	546		
B	REAL	19200		/SECOND/
BB	REAL	562		
BOT	REAL	12800		/THIRD /
BOTT	REAL	374		
CC	REAL	574		
D	REAL	438		
DD	REAL	566		
DELTA	REAL	330		
DELX	REAL	19200		/THIRD /
DEY	REAL	19360		/THIRD /
I	REAL	390		
DEY	REAL	394		



Microsoft FORTRAN77 V3.30 March 1985

```

D Line# 1      7
DL      REAL      12800    /SECOND/
E      REAL      450
F      REAL      334
G      REAL      442
FN1     CHAR*64      54
FN2     CHAR*64     165
FN3     CHAR*64     262
G      REAL     19360    /SECOND/
H      REAL        0    /FIRST /
HA      REAL      590
HH      REAL      354
HD      REAL     6400    /FIRST /
I      INTEGER*4     382
II      INTEGER*4     550
ISTEP   INTEGER*4     422
ITER    INTEGER*4     446
J      INTEGER*4     402
JJ      INTEGER*4     606
MAXIT   INTEGER*4     378
MOD                      INTRINSIC
N      INTEGER*4     586
NC      INTEGER*4     338
NR      INTEGER*4     342
NRG     INTEGER*4     366
NSTEPS  INTEGER*4     326
PERM    REAL        0    /THIRD /
PP      REAL      370
Q      REAL     19200    /FIRST /
QQ      REAL      358
S2      REAL      350
SF2     REAL     12800    /FIRST /
SQRT                      INTRINSIC
T      REAL        0    /SECOND/
TIME    REAL      418
TMULT   REAL      362
TT      REAL      346
W      REAL      578
WW      REAL      582

```

Name	Type	Size	Class
FIRST		25600	COMMON
MAIN			PROGRAM
SECOND		19520	COMMON
THIRD		19520	COMMON

Pass One No Errors Detected  
262 Source Lines

D:\SLOPE\PLASM> type p3.dat  
0.933 1.0 5 10 74.79 1.112 400 0 1.2 0 3.74 0  
20

D:\SLOPE\PLASM>

type p3.dat

25 0.933 1.0 5 10 74.79 1.112 400 0 1.2 0 3.74 0  
20 20

D:\SLOPE\PLASM> type p3.prn

1	1	74.79	74.79	210	-400.9	1.0E+30	3.74	3.74	190
1	2	74.79	74.79	190	-400.9	2.244	3.74	3.74	170
1	3	74.79	74.79	170	-400.9	2.244	3.74	3.74	150
1	4	74.79	74.79	150	-400.9	2.244	3.74	3.74	130
1	5	74.79	74.79	130	-400.9	2.244	3.74	3.74	110
1	6	74.79	74.79	110	-400.9	2.244	3.74	3.74	90
1	7	74.79	74.79	90	-400.9	2.244	3.74	3.74	70
1	8	74.79	74.79	70	-400.9	2.244	3.74	3.74	50
1	9	74.79	74.79	50	-400.9	2.244	3.74	3.74	30
1	10	74.79	74.79	30	-400.9	1.0E+30	3.74	3.74	10
2	1	74.79	74.79	210	-400.9	1.0E+30	3.74	3.74	190
2	2	74.79	74.79	190	-400.9	2.244	3.74	3.74	170
2	3	74.79	74.79	170	-400.9	2.244	3.74	3.74	150
2	4	74.79	74.79	150	-400.9	2.244	3.74	3.74	130
2	5	74.79	74.79	130	-400.9	2.244	3.74	3.74	110
2	6	74.79	74.79	110	-400.9	2.244	3.74	3.74	90
2	7	74.79	74.79	90	-400.9	2.244	3.74	3.74	70
2	8	74.79	74.79	70	-400.9	2.244	3.74	3.74	50
2	9	74.79	74.79	50	-400.9	2.244	3.74	3.74	30
2	10	74.79	74.79	30	-400.9	1.0E+30	3.74	3.74	10
3	1	74.79	74.79	210	-400.9	1.0E+30	3.74	3.74	190
3	2	74.79	74.79	190	-400.9	2.244	3.74	3.74	170
3	3	74.79	74.79	170	-400.9	2.244	3.74	3.74	150
3	4	74.79	74.79	150	-400.9	2.244	3.74	3.74	130
3	5	74.79	74.79	130	-400.9	2.244	3.74	3.74	110
3	6	74.79	74.79	110	-400.9	2.244	3.74	3.74	90
3	7	74.79	74.79	90	-400.9	2.244	3.74	3.74	70
3	8	74.79	74.79	70	-400.9	2.244	3.74	3.74	50
3	9	74.79	74.79	50	-400.9	2.244	3.74	3.74	30
3	10	74.79	74.79	30	-400.9	1.0E+30	3.74	3.74	10
4	1	74.79	74.79	210	-400.9	1.0E+30	3.74	3.74	190
4	2	74.79	74.79	190	-400.9	2.244	3.74	3.74	170
4	3	74.79	74.79	170	-400.9	2.244	3.74	3.74	150
4	4	74.79	74.79	150	-400.9	2.244	3.74	3.74	130
4	5	74.79	74.79	130	-400.9	2.244	3.74	3.74	110
4	6	74.79	74.79	110	-400.9	2.244	3.74	3.74	90
4	7	74.79	74.79	90	-400.9	2.244	3.74	3.74	70
4	8	74.79	74.79	70	-400.9	2.244	3.74	3.74	50
4	9	74.79	74.79	50	-400.9	2.244	3.74	3.74	30
4	10	74.79	74.79	30	-400.9	1.0E+30	3.74	3.74	10
5	1	74.79	74.79	210	-400.9	1.0E+30	3.74	3.74	190
5	2	74.79	74.79	190	-400.9	2.244	3.74	3.74	170
5	3	74.79	74.79	170	-400.9	2.244	3.74	3.74	150
5	4	74.79	74.79	150	-400.9	2.244	3.74	3.74	130
5	5	74.79	74.79	130	-400.9	2.244	3.74	3.74	110
5	6	74.79	74.79	110	-400.9	2.244	3.74	3.74	90
5	7	74.79	74.79	90	-400.9	2.244	3.74	3.74	70
5	8	74.79	74.79	70	-400.9	2.244	3.74	3.74	50
5	9	74.79	74.79	50	-400.9	2.244	3.74	3.74	30
5	10	74.79	74.79	30	-400.9	1.0E+30	3.74	3.74	10

**APPENDIX D**  
**PROGRAM "SWAP"**

```

D Line# 1      7      Microsoft FORTRAN77 V3.30 March 1985
1 C*****
2 C
3 C      PROGRAM "MATRIX": TRANSFORMS MAP OF FLOW MODEL HEAD VALUES
4 C      INTO AN XYZ FORMAT FOR GRAPHING.
5 C
6 C      C.R. PETRICH
7 C      1988
8 C
9 C*****
10 C
11 C      DEFINITION OF VARIABLES
12 C
13 C      NR = NUMBER OF ROWS
14 C      NC = NUMBER OF COLUMNS
15 C      H = TEMPORARY HEAD VALUE
16 C      IY = NUMBER OF ROWS, WITH ORIGIN AT LOWER LEFT CORNER
17 C      HMAP = HEAD ARRAY WITH ORIGIN IN UPPER LEFT CORNER
18 C      FX = MULTIPLICATION FACTOR IN THE X DIRECTION
19 C      FY = MULTIPLICATION FACTOR IN THE Y DIRECTION
20 C      TC & TR = TEMPORARY COLUMN AND ROW VARIABLES
21 C
22 C      NOTE: IF NC, NR > 20, CHANGE FORMATS FOR WRITE STATEMENTS
23 C
24 C*****
25 C
26 C      INTEGER I,J
27 C      REAL H, FX, FY, IY, TC, TY
28 C      DIMENSION HEAD (50,50), HMAP (50,50), HNEW (50,50)
29 C      CHARACTER*15 IFILE, OFILE, OGFILE
30 C      WRITE (*,10)
31 C      WRITE (*,10) '*****'
32 C      WRITE (*,10)
33 C      WRITE (*,10) ' THIS PROGRAM TRANSFORMS HEAD OR CONCENTRATION
34 C      WRITE (*,10) ' VALUES FROM MATRIX FORM INTO AN XYZ FORMAT FOR
35 C      WRITE (*,10) ' GRAPHING. A MULTIPLICATION FACTOR IS REQUESTED
36 C      WRITE (*,10) ' FOR SITUATIONS WHERE DELTA X DOES NOT EQUAL
37 C      WRITE (*,10) ' DELTA Y.
38 C      WRITE (*,10)
39 C      WRITE (*,10) '*****'
40 C      WRITE (*,10)
41 C      WRITE (*,10) ' ENTER NAME OF INPUT FILE:
42 10  FORMAT (A)
43 C      READ (*,10) IFILE
44 C      OPEN (5,FILE=IFILE)
45 C      WRITE (*,10) ' ENTER NAME OF OUTPUT FILE (.SWP):
46 C      READ (*,10) OFILE
47 C      OPEN (6,FILE=OFILE,STATUS='NEW')
48 C      WRITE (*,10) ' ENTER NAME OF GRAPHING OUTPUT FILE (.DAT):
49 C      READ (*,10) OGFILE
50 C      OPEN (7, FILE=OGFILE,STATUS='NEW')
51 C
52 C      ENTER DATA
53 C
54 C      WRITE (*,20)
55 20  FORMAT (' ENTER THE NUMBER OF COLUMNS: ')
56 C      READ (*,*) NC

```

```

D Line# 1      7      Microsoft FORTRAN77 V3.30 March 1985
  57      WRITE (*,30)
  58 30      FORMAT (' ENTER THE NUMBER OF ROWS: ')
  59      READ (*,*) NR
  60 C
  61 C      ENTER MULTIPLICATION FACTORS FOR X AND Y GRID BLOCKS
  62 C
  63      WRITE (*,31)
  64 31      FORMAT (' ENTER MULTIPLICATION FACTOR FOR X DIRECTION: ')
  65      READ (*,*) FX
  66      WRITE (*,32)
  67 32      FORMAT (' ENTER MULTIPLICATION FACTOR FOR Y DIRECTION: ')
  68      READ (*,*) FY
  69 C
  70 C      READ AND PRINT HEAD MATRIX
  71 C
  72      DO 50 I=1,NR
1  73      READ (5,*) (HMAP(I,J),J=1,NC)
1  74      WRITE (6,40) (HMAP(I,J),J=1,NC)
1  75 40      FORMAT (/ ,1X,20(F5.2,1X))
1  76 50      CONTINUE
  77 C
  78 C      INVERT Y-AXIS OF HEAD MATRIX, PRINT XYZ HEAD DATA TO GRAPH FILE
  79 C
  80      IY=NR
  81      DO 90 I=1,NR
2  82      DO 80 J=1,NC
2  83      TC=J*FX
2  84      TR=IY*FY
2  85      WRITE (7,70) TC,TR,HMAP(I,J)
2  86 70      FORMAT (F5.2,1X,F5.2,1X,F10.2)
2  87      IY=TR/FY
2  88 80      CONTINUE
1  89      IY=IY-1
1  90 90      CONTINUE
  91      STOP
  92      END

```

Name	Type	Offset P Class
FX	REAL	30194
FY	REAL	30250
H	REAL	*****
HEAD	REAL	16
HMAP	REAL	10016
HNEW	REAL	20016
I	INTEGER*4	30254
IFILE	CHAR*15	30020
IY	REAL	30290
J	INTEGER*4	30262
NC	INTEGER*4	30102
NR	INTEGER*4	30138
OFIIE	CHAR*15	30035
OFIIE	CHAR*15	30050
TC	REAL	30302
TR	REAL	30306
TY	REAL	*****

D Line# 1 7

Microsoft FORTRAN77 V3.30 March 1985

93  
94  
95  
96  
97  
98  
99  
100  
101  
102

Name	Type	Size	Class
MAIN			PROGRAM

Pass One      No Errors Detected  
              102 Source Lines

D:\TEMP&gt;

PLASM Data Sheet

					Column	Row	T(x)	T(y)	Initial Head	Storage Recharge	Factor	K(x)	K(y)	Bottom Elev.
TRANSMISSIVITY					1	1	37.4	37.4	200	100.22	1E+30	3.74	3.74	190
37.4	37.4	37.4	37.4	37.4	1	2	37.4	37.4	180	100.22	1.122	3.74	3.74	170
37.4	37.4	37.4	37.4	37.4	1	3	37.4	37.4	160	100.22	1.122	3.74	3.74	150
37.4	37.4	37.4	37.4	37.4	1	4	37.4	37.4	140	100.22	1.122	3.74	3.74	130
37.4	37.4	37.4	37.4	37.4	1	5	37.4	37.4	120	100.22	1.122	3.74	3.74	110
37.4	37.4	37.4	37.4	37.4	1	6	37.4	37.4	100	100.22	1.122	3.74	3.74	90
37.4	37.4	37.4	37.4	37.4	1	7	37.4	37.4	80	100.22	1.122	3.74	3.74	70
37.4	37.4	37.4	37.4	37.4	1	8	37.4	37.4	60	100.22	1.122	3.74	3.74	50
37.4	37.4	37.4	37.4	37.4	1	9	37.4	37.4	40	100.22	1.122	3.74	3.74	30
37.4	37.4	37.4	37.4	37.4	1	10	37.4	37.4	20	100.22	1E+30	3.74	3.74	10
37.4	37.4	37.4	37.4	37.4	2	1	37.4	37.4	200	100.22	1E+30	3.74	3.74	190
Aquifer thickness 10 ft					2	2	37.4	37.4	180	100.22	1.122	3.74	3.74	170
					2	3	37.4	37.4	160	100.22	1.122	3.74	3.74	150
					2	4	37.4	37.4	140	100.22	1.122	3.74	3.74	130
					2	5	37.4	37.4	120	100.22	1.122	3.74	3.74	110
					2	6	37.4	37.4	100	100.22	1.122	3.74	3.74	90
					2	7	37.4	37.4	80	100.22	1.122	3.74	3.74	70
					2	8	37.4	37.4	60	100.22	1.122	3.74	3.74	50
					2	9	37.4	37.4	40	100.22	1.122	3.74	3.74	30
					2	10	37.4	37.4	20	100.22	1E+30	3.74	3.74	10
INITIAL HEAD VALUES INCR: 20					3	1	37.4	37.4	200	100.22	1E+30	3.74	3.74	190
200	200	200	200	200	3	2	37.4	37.4	180	100.22	1.122	3.74	3.74	170
180	180	180	180	180	3	3	37.4	37.4	160	100.22	1.122	3.74	3.74	150
160	160	160	160	160	3	4	37.4	37.4	140	100.22	1.122	3.74	3.74	130
140	140	140	140	140	3	5	37.4	37.4	120	100.22	1.122	3.74	3.74	110
120	120	120	120	120	3	6	37.4	37.4	100	100.22	1.122	3.74	3.74	90
100	100	100	100	100	3	7	37.4	37.4	80	100.22	1.122	3.74	3.74	70
80	80	80	80	80	3	8	37.4	37.4	60	100.22	1.122	3.74	3.74	50
60	60	60	60	60	3	9	37.4	37.4	40	100.22	1.122	3.74	3.74	30
40	40	40	40	40	3	10	37.4	37.4	20	100.22	1E+30	3.74	3.74	10
20	20	20	20	20	4	1	37.4	37.4	200	100.22	1E+30	3.74	3.74	190
PUMPING RATE (RECHARGE)					4	2	37.4	37.4	180	100.22	1.122	3.74	3.74	170
100.22	100.22	100.22	100.22	100.22	4	3	37.4	37.4	160	100.22	1.122	3.74	3.74	150
100.22	100.22	100.22	100.22	100.22	4	4	37.4	37.4	140	100.22	1.122	3.74	3.74	130
100.22	100.22	100.22	100.22	100.22	4	5	37.4	37.4	120	100.22	1.122	3.74	3.74	110
100.22	100.22	100.22	100.22	100.22	4	6	37.4	37.4	100	100.22	1.122	3.74	3.74	90
100.22	100.22	100.22	100.22	100.22	4	7	37.4	37.4	80	100.22	1.122	3.74	3.74	70
100.22	100.22	100.22	100.22	100.22	4	8	37.4	37.4	60	100.22	1.122	3.74	3.74	50
100.22	100.22	100.22	100.22	100.22	4	9	37.4	37.4	40	100.22	1.122	3.74	3.74	30
100.22	100.22	100.22	100.22	100.22	4	10	37.4	37.4	20	100.22	1E+30	3.74	3.74	10
SF2					5	1	37.4	37.4	200	100.22	1E+30	3.74	3.74	190
1E+30	1E+30	1E+30	1E+30	1E+30	5	2	37.4	37.4	180	100.22	1.122	3.74	3.74	170
1.122	1.122	1.122	1.122	1.122	5	3	37.4	37.4	160	100.22	1.122	3.74	3.74	150
1.122	1.122	1.122	1.122	1.122	5	4	37.4	37.4	140	100.22	1.122	3.74	3.74	130
1.122	1.122	1.122	1.122	1.122	5	5	37.4	37.4	120	100.22	1.122	3.74	3.74	110
1.122	1.122	1.122	1.122	1.122	5	6	37.4	37.4	100	100.22	1.122	3.74	3.74	90
1.122	1.122	1.122	1.122	1.122	5	7	37.4	37.4	80	100.22	1.122	3.74	3.74	70
1.122	1.122	1.122	1.122	1.122	5	8	37.4	37.4	60	100.22	1.122	3.74	3.74	50
1.122	1.122	1.122	1.122	1.122	5	9	37.4	37.4	40	100.22	1.122	3.74	3.74	30
1.122	1.122	1.122	1.122	1.122	5	10	37.4	37.4	20	100.22	1E+30	3.74	3.74	10
1.122	1.122	1.122	1.122	1.122										
1.122	1.122	1.122	1.122	1.122										
1E+30	1E+30	1E+30	1E+30	1E+30										
PERM1														
3.74	3.74	3.74	3.74	3.74										
3.74	3.74	3.74	3.74	3.74										
3.74	3.74	3.74	3.74	3.74										
3.74	3.74	3.74	3.74	3.74										
3.74	3.74	3.74	3.74	3.74										
3.74	3.74	3.74	3.74	3.74										

Table 3.2-1  
Lotus 1-2-3 Worksheet for PLASM Model

3.74	3.74	3.74	3.74	3.74
3.74	3.74	3.74	3.74	3.74
3.74	3.74	3.74	3.74	3.74
3.74	3.74	3.74	3.74	3.74

ERM2

3.74	3.74	3.74	3.74	3.74
3.74	3.74	3.74	3.74	3.74
3.74	3.74	3.74	3.74	3.74
3.74	3.74	3.74	3.74	3.74
3.74	3.74	3.74	3.74	3.74
3.74	3.74	3.74	3.74	3.74
3.74	3.74	3.74	3.74	3.74
3.74	3.74	3.74	3.74	3.74
3.74	3.74	3.74	3.74	3.74
3.74	3.74	3.74	3.74	3.74

BOTTOM ELEVATIONS

INCR:

20

190	190	190	190	190
170	170	170	170	170
150	150	150	150	150
130	130	130	130	130
110	110	110	110	110
90	90	90	90	90
70	70	70	70	70
50	50	50	50	50
30	30	30	30	30
10	10	10	10	10



## **ATTACHMENT 4**

## A Temporal Model for Landslide Risk Based on Historical Precipitation<sup>1</sup>

Stanley M. Miller<sup>2</sup>

---

*Of the recognized nonsteady-state factors that influence slope stability, probably most critical in many field situations is the character of precipitation and infiltration activity. A groundwater response model used in conjunction with precipitation records can provide a historical catalog of estimated maximum groundwater levels in a particular study area. An extreme-value statistical analysis of this catalog is linked with geotechnical slope stability analyses to provide a landslide hazard model for estimating the probability of slope failure within a given time. This modeling approach can provide meaningful input to risk assessments for landslide mitigation programs and to decision analyses and cost-benefit studies important for land-use planning and resource management.*

---

**KEY WORDS:** slope stability, landslide hazards, extreme-value statistics, Monte Carlo simulation.

### INTRODUCTION

Time-dependent factors that influence the stability of natural slopes include rock weathering, soil development, surface erosion (and its relationship with vegetation cover), creep-induced reduction in shear strength, and the character of precipitation activity. For typical time spans associated with land-use planning and resource management (usually less than 75 yr), the most critical of these factors is precipitation activity. Although precipitation will affect vegetation cover and erosion characteristics, its major influence on slope stability in steep mountainous terrain of the Western U.S. is the near-surface groundwater response.

Many landslides induced by such activity occur in a relatively shallow soil mantle (.5 m to 8 m thick) that blankets bedrock hillslopes. Precipitation infiltrates faster than the subsurface water can percolate into the underlying bedrock. Consequently, a perched phreatic surface forms within the soil mantle (which,

---

<sup>1</sup>This paper was presented at Emerging Concepts, MGUS 87 Conference, Redwood City, California, 13-15 April 1987. Manuscript received 15 April 1987; accepted 27 May 1987.

<sup>2</sup>Department of Geology and Geological Engineering, University of Idaho, Moscow, Idaho 83843.

in most cases, is a mixture of soil, colluvium, and extensively weathered bedrock). This rise in the near-surface groundwater level induces pore and seepage pressures that may lead to unstable conditions and landslides. In the case of existing, relatively slow-moving landslides, the rise in phreatic surface may reactivate or accelerate movement of the slide mass. In other cases, formerly stable slope segments may rapidly mobilize into fast-moving, violent debris flows that strip the soil mantle and its associated vegetation from the sloping bedrock surface.

Land-use planning and resource management could be enhanced by time-based predictions of slope stability. Current landslide research at the University of Idaho concentrates on probabilistic stability analyses that can incorporate historical precipitation information into groundwater response and slope stability models. This approach leads to time-based estimates of the probability of slope failures.

### Geotechnical Considerations

An accepted geotechnical engineering approach for slope stability investigations consists of applying proven two-dimensional, limiting-equilibrium stability models to potential failure geometries that have been identified in the slope. The output of such an analysis is the calculated factor of safety, which is the ratio of resisting forces to driving forces. Input data for slope stability analyses include material properties, such as unit weight and shear strength, and site conditions, such as slope angle, boundaries of geologic units, and height of the phreatic surface. Uncertainties in values of these input properties arise from stochastic variability, which is tied to natural spatial variability and to measurement errors, and from lack of knowledge about the physical system being analyzed. Many uncertainties can be accounted for in a probabilistic slope stability analysis (Miller, 1984; Kirsten and Moss, 1985). Each of the pertinent input properties is treated as a random variable described by a defined probability density function (pdf), where definition is based on field observations, laboratory test results, or professional judgment.

Several computational methods are available for inserting these pdf's into the selected limiting equilibrium equation in order to estimate the pdf of the factor of safety. The most commonly used technique is Monte Carlo simulation, wherein repeated sampling of possible sets of input values leads to repeated calculations of possible safety factor values. The percentage of simulated safety factor values that are less than 1 (a safety factor of 1 indicates limiting equilibrium) is an estimate of the probability of slope failure. Although such procedures incorporate the uncertainties and even perhaps the interdependence of input properties, they cannot include temporal fluctuations in groundwater conditions unless time-dependent pdf's of water levels can be estimated.

### Hazard Assessment Vs. Risk Analysis

In the context of the following discussions, a landslide hazard assessment (also known as a slope reliability analysis) consists of using probabilistic models to deduce in a quantified manner the uncertainties associated with predictions of slope stability. These uncertainties typically are bundled into an estimate of slope instability, known as the probability of slope failure. If similar slope segments within a given geomorphic unit (or land-type unit) have an estimated probability of failure equal to 0.30, the slope reliability is 0.70. The probability of failure value commonly is obtained by a Monte Carlo simulation overlay on the safety factor equation. By repeating the probabilistic analysis for the various land-type units in a region, an areal distribution of quantified landslide hazards can be generated.

The results of such a landslide hazard assessment can be incorporated into a socioeconomic framework to provide a system for evaluating pertinent social or economic risks, where the term "risk" implies susceptibility to losses. The development and implementation of such a system is known as a risk analysis. Whereas a hazard assessment is conducted primarily by scientists and engineers, a risk analysis is influenced heavily by managers, planners, politicians, and the general public.

Landslide hazard assessment differs from risk analysis. Two areas may have similar estimates of predicted hazard but entirely different risks. For example, the slopes in two different land-type areas may have similar probability of failure values, but one of the areas may have a much greater associated risk due to a greater potential for losing an important transportation route, recreational benefits, or natural resources such as timber.

### THEORETICAL BACKGROUND AND ASSUMPTIONS

Many landslides that occur in steep mountainous terrain consist of a translational movement of part or all of the soil mantle that blankets the bedrock slopes. Even the wet, fluid-type debris flows probably are characterized by a brief initial translational displacement before they become turbid flows. An appropriate analytical model for such failures is the infinite slope model described by Ward et al. (1979). Part of the input to this model, which is condensed into an equation for the limiting equilibrium safety factor, is the height of the phreatic surface in the soil mantle.

The statistical theory of extreme values (Gumbel, 1958) provides a convenient method for characterizing temporal fluctuations of the water levels, so that the stochastic behavior of the water surface over time can be incorporated into the slope stability analysis. This approach relies on historical records of extreme (maximum) values estimated for water levels. Particular emphasis on

extreme values is especially relevant to landslide studies, because slope instabilities are most likely to occur when groundwater levels are highest. Therefore, predicting the highest water level that could occur within a given time period is more important than describing random fluctuations in water levels over the time period.

### Stability Analysis Based on the Infinite Slope Model

The infinite slope model considers the limiting equilibrium of a two-dimensional soil element that has unit thickness and unit width (Fig. 1). Physical conditions in the slope are assumed to be infinitely constant in the upslope and downslope directions. The factor of safety is calculated as follows (Ward et al., 1979)

$$FS = \frac{C_r + \tau}{\sin B \cos B [q_0 + \gamma(H - H_w) + \gamma_{sat}H_w]} \quad (1)$$

where  $B$  = slope angle,  $H$  = depth of soil,  $H_w$  = height of phreatic surface in the soil,  $C_r$  = cohesion due to tree roots,  $\tau$  = shear strength of soil,  $q_0$  = surcharge due to weight of trees,  $\gamma$  = natural unit weight of soil,  $\gamma_{sat}$  = saturated unit weight of soil.

The shear strength is a physical property of the soil that depends on the applied effective normal stress. It is measured through laboratory or field tests and almost always is represented as a linear or power function of the effective normal stress. Miller and Borgman (1984) suggested one method to characterize the shear strength in a probabilistic framework. The other input terms in Eq.

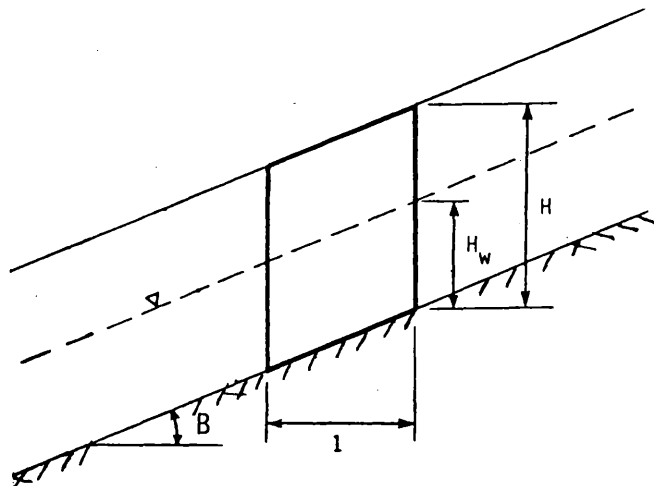


Fig. 1. Infinite slope model used for slope stability calculations.

(1) can be treated as constants or as random variables described by appropriate pdf's.

The input of major concern to this discussion is the height of the phreatic surface. Most mountainous regions have an annual wet season when abundant water infiltration significantly elevates the near-surface groundwater levels. This period is associated with rainy seasons or with spring snow-melt activity. Groundwater monitoring by the U.S. Forest Service in the North-Central Rockies has indicated that shallow phreatic surfaces in typical mountainous areas tend to be stable except during the spring months when significant rises are observed (Prellwitz and Babbitt, 1984). Consequently, the input pdf of water height for the safety factor equation should not reflect daily or weekly fluctuations, but rather the maximum heights that can be expected annually. Such input would be exceedingly useful for a time-based evaluation of landslide hazard.

### Extreme-Value Statistical Analysis

Extreme-value statistical methods are appropriate for dealing with groundwater levels in a geotechnical analysis of slope stability. The Type 1 maximum-value distribution (Gumbel, 1958) has wide applicability because it is based on the assumption that the random variable of interest has a probability distribution whose right tail is unbounded and is of an exponential type, which includes important pdf's such as normal, lognormal, and gamma probability functions. Another important assumption for the Type 1 distribution is that the original stochastic process must consist of a collection of these random variables that are independent and identically distributed.

In this case, groundwater levels comprise the stochastic process, and the random variables  $X_i$  (for  $i = 1, 2, \dots, n$ ) denote the  $i$ th water level of  $n$  water levels occurring in a year. If the  $X_i$  are independent and identically distributed as described above, the cumulative distribution function of  $Y$ , the annual maximum water level, is given by the Type 1 maximum-value distribution (Soong, 1981, p. 221)

$$F(y) = \exp \left\{ -\exp [-a(y - u)] \right\} \quad \text{for} \quad -\infty < y < \infty \quad (2)$$

where  $a (>0)$  and  $u$  are the two parameters of the distribution. Various applications of this maximum-value distribution to problems in engineering, climatology, hydrology, and other fields were presented by Kinnison (1985). Carr and Bailey (1986) recently discussed and evaluated extreme-value methods for assessing earthquake hazards. Near-surface groundwater levels can be treated in the same extreme-value context as river floods, wind gusts, earthquakes, and other naturally occurring temporal phenomena.

Equation (2) can be used to calculate the probability that the annual maximum will not exceed a specified threshold level  $y'$ . If this probability is tied to

a specified time interval in years, the following expression is obtained

$$P(Y \leq y') = \exp \left\{ -T \cdot \exp \left[ -a(y' - u) \right] \right\} \quad (3)$$

where  $y'$  = threshold value of maximum water level,  $T$  = time interval in years,  $a = S_n/s_y$ , and  $u = m_y - (M_n/a)$ . (4) and (5)

The terms  $m_y$  and  $s_y$  are mean and standard deviation of the annual maximum values shown in the historical record (catalog of  $n$  years). The terms  $M_n$  and  $S_n$  are mean and standard deviation of Gumbel's reduced extremes; they depend on  $n$  (total number of years in the historical record) and are tabulated accordingly by Gumbel (1958, p. 228).

### TIME-DEPENDENT HAZARD ASSESSMENT FOR LANDSLIDES

Monte Carlo simulation applied to the infinite slope equation [Eq. (1)] can be used to estimate the probability of slope failure over a given time. The temporal input to the analysis consists of time-dependent pdf's of the annual maximum height of the phreatic surface. These pdf's are estimated by using Eq. (3) in conjunction with a history of annual maximum groundwater levels in the study area. Unfortunately, this historical information hardly ever is available directly because long-term (e.g., 30–50 yr) phreatic-surface monitoring of this type is rare. Even in recognized landslide-prone areas where groundwater levels have been monitored, the historical records are incomplete and do not extend over periods longer than 5 or 6 yr.

Historical information on water levels must be obtained indirectly. A reasonable approach relies on recharge and groundwater-response modeling based on historical precipitation records, which usually are available for the study area or for nearby areas. Sangrey et al. (1984) have proposed a groundwater response model wherein the height of the phreatic surface is assumed to be linearly related to the effective recharge at a specific study site. Linear regression coefficients are calculated by a regression of known water levels recorded during a given time period against calculated values of effective recharge over the same period of record. The effective recharge values are estimated by a time-dependent equation that considers evapotranspiration and the drainage time of the slope unit; this equation is solved iteratively to provide effective recharge values necessary for the linear regression over the calibration period. Conceivably, once this model is calibrated for the site, it can be applied to the longer-term precipitation records to indirectly estimate the annual maximum rises in the local phreatic surface.

Finite-element and finite-difference computer codes, such as UNSAT2 (Neuman et al., 1974) and PLASM (Prickett and Lonquist, 1971), also can be used to approximate the maximum rise in the phreatic surface associated

with precipitation and recharge. Input data requirements are more extensive for these models than for the regression/calibration method described previously. Minimal hydrogeologic information necessary to use these computer codes includes hydraulic conductivity, porosity, storage coefficient, appropriate boundary conditions, and good physical descriptions of the site geometry. The models can be calibrated and/or verified by several years of water-level measurements, most of which should be taken during the wet season.

Research efforts at the University of Idaho are continuing to evaluate and refine the above methods for estimating groundwater response to precipitation/recharge events for soil mantles on sloping bedrock surfaces. The goal is to provide a reasonably accurate time history of maximum annual heights of the phreatic surface at specific study sites.

A catalog of maximum annual water levels is the key input to an extreme-value analysis that provides time-dependent cdf's of the maximum annual water levels. Basic steps in the analysis are outlined below:

1. Calculate sample mean ( $m_y$ ) and standard deviation ( $s_y$ ) from the historical listing of  $n$  maximum annual water levels.
2. Identify mean and standard deviation of the reduced extremes for  $n$  years ( $M_n$  and  $S_n$ , respectively) from Gumbel's table (1958, p. 228).
3. Calculate parameters of the Type 1 maximum-value distribution ( $a$  and  $u$ ) using Eqs. (4) and (5).
4. Estimate the cdf of maximum annual water levels for a given time  $T$  by selecting a series of threshold values ( $y'$ ) and by calculating the probabilities according to Eq. (3).
5. Repeat step 4 for as many different periods as needed.

In many cases, working with a water height ratio ( $H_w/H$ ) may be more convenient than actual water height. This approach allows for generic comparisons among different sites with varying thicknesses of soil mantles. Results of a typical extreme-value analysis indicate that the maximum annual water height ratio has a greater chance of taking on larger values as the time period increases (Fig. 2).

An example will serve to illustrate the overall, time-based hazard assessment for landslides. Consider a hypothetical land-type unit that has the following characteristics:

Soil mantle depth,  $H$ : Uniformly distributed from 12 to 17 ft (3.66–5.18 m)

Slope (percent grade): Uniformly distributed from 33 to 43 %

Tree surcharge and root cohesion are negligible

Shear strength is a linear function of effective normal stress with  $y$  intercept equal to 36 psf (0.176 tsm) and a slope of 0.532.



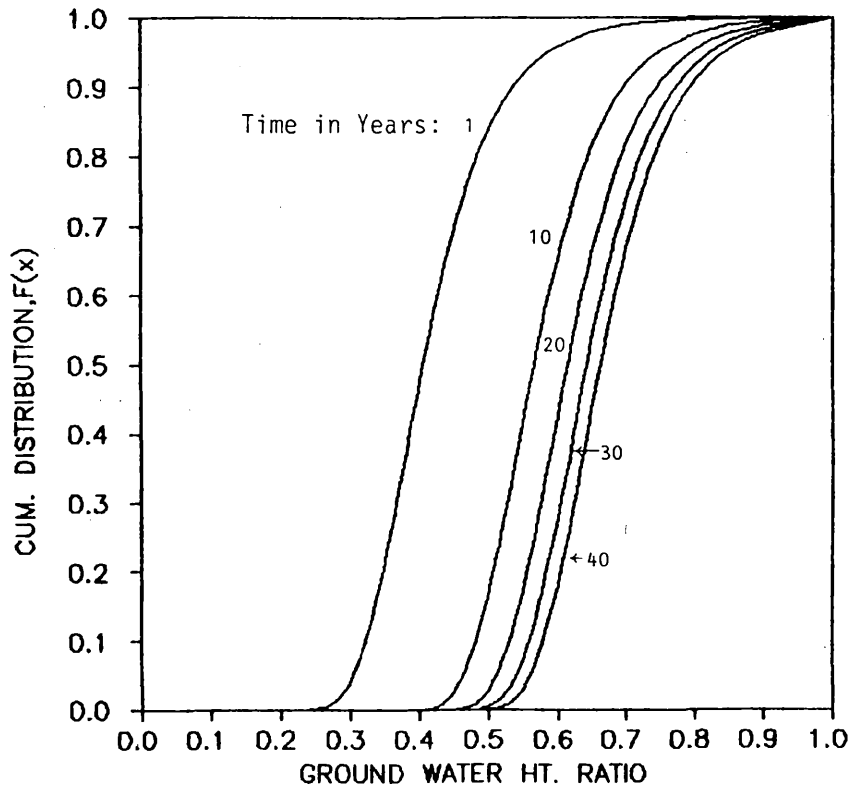


Fig. 2. Time-dependent cdf's of maximum annual groundwater height ratio for a 47-yr record ( $M_n = 0.5473$ ,  $S_n = 1.1557$ ;  $m_y = 0.42$ ,  $s_y = 0.02$ ).

Soil natural unit weight and saturated unit weight are calculated from the following input information:

Dry unit weight is normally distributed with mean 100 pcf (1.60 tcm) and with S.D. 3 pcf (0.05 tcm).

Moisture content is normally distributed with mean 15% and S.D. 2%.

Time-dependent probability distributions of groundwater levels are given by the cdf's in Fig. 2.

A Monte Carlo simulation based on the infinite slope model [Eq. (1)] provides time-based probability of failure values (Fig. 3). Simulated values of the safety factor are either normally distributed or skewed slightly to the right (an example histogram is shown in Fig. 4). This example is based on a historical precipitation record that covers the period from 1938 through 1985 (47 yr).

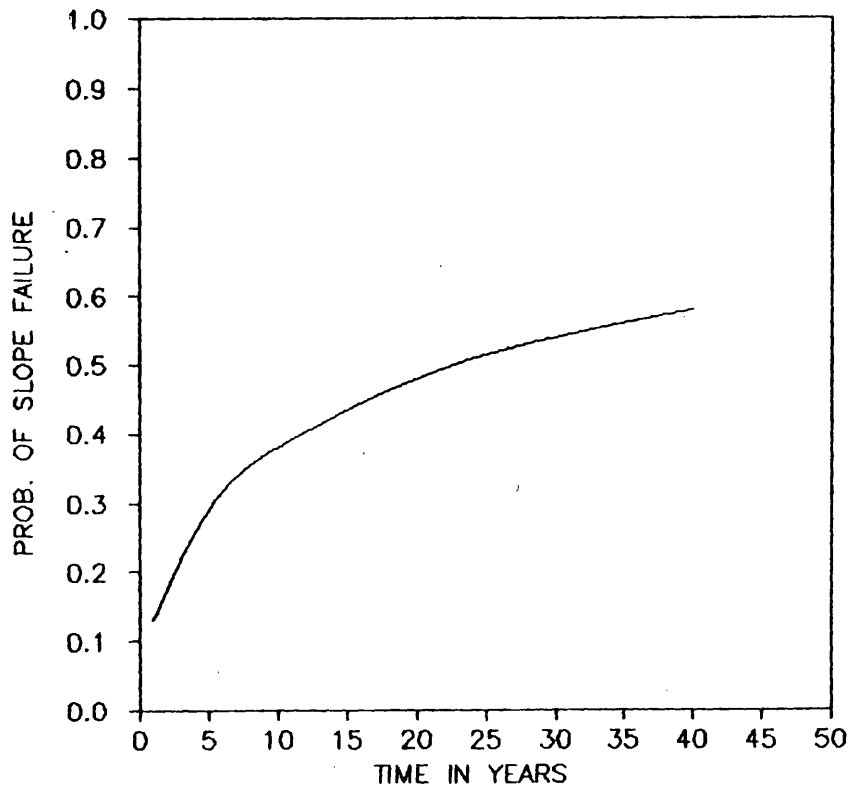


Fig. 3. Temporal values of probability of slope failure for example problem.

This length of record limits the landslide hazard assessment to a maximum projected period of approximately 30 yr.

#### RISK ASSESSMENT AND DECISION ANALYSIS

Time-based probabilistic output, such as that obtained from the Monte Carlo simulation example above, provides essential information for a thorough landslide risk analysis. In resource management and land-use planning applications, a risk assessment typically has a logical extension into decision analysis, where the evaluated risks of various alternatives are compared to provide assistance in decision-making. Therefore, some kind of values, monetary or otherwise, must be placed on consequences of the decision alternatives; this is where risks are incorporated.

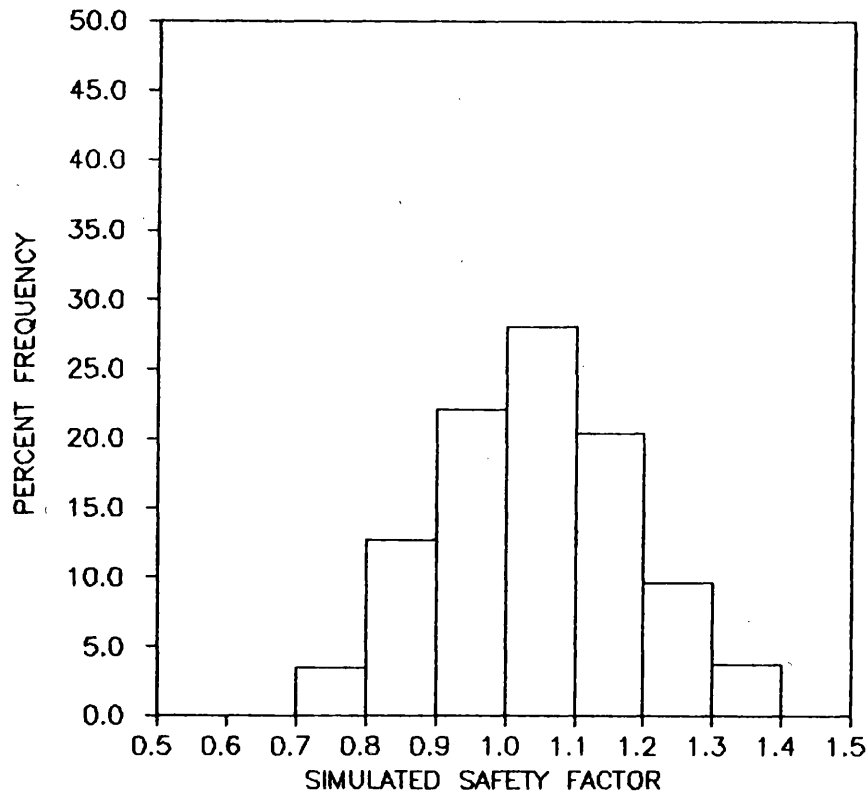


Fig. 4. Histogram of 1000 simulated values of safety factor ( $T = 10$  yr).

The use of expected monetary value (EMV) as a comparative index is one common approach to decision analysis. In the case of landslide risk analysis, the EMV is a measure of risk and is defined as the product obtained by multiplying the probability of a landslide occurring by the conditional value (economic loss) incurred if the landslide occurs. In general, the EMV of a decision alternative is the algebraic sum of the EMV's of all possible outcomes that could occur if that alternative is selected. Decision makers should follow a consistent behavior of always selecting the alternative with the highest EMV (Newendorp, 1975).

As a practical example, consider a simple problem in forest management: deciding which one of two potential timber cutting areas should be harvested. The areas are similar in size but located in different land types; only one of them will be harvested in order to minimize visual and recreational impacts. Assuming that the selected harvest area will be clearcut, a time-based landslide risk assessment is especially appropriate because a period of negligible tree

surcharge and root cohesion is initiated at harvest. These conditions likely will persist for 30 to 40 yr until significant timber regeneration will restore the hill-slope to its natural condition. Two decision alternatives exist: (1) to harvest Area A, (2) to harvest Area B; each of these alternatives has two mutually exclusive outcomes, either a landslide occurs or a landslide does not occur.

Reasonable benefits and costs (in today's dollars) for the two hypothetical harvesting areas are estimated as

	Area A	Area B
Timber value (in \$1000)	1320	1410
Value assigned to landslide impacts (in \$1000) including road reconstruction, increased re- generation time, sedimentation damage to streams, other visual/recreational damage	-1550	-1980

An extreme-value statistical analysis, based on historical precipitation records linked to a groundwater response model, is used to provide time-dependent cdf's of the maximum annual groundwater levels for each of the potential harvesting areas. These cdf's are input to a Monte Carlo version of the infinite slope, safety-factor model to generate time-dependent probability of failure values for the two areas (Fig. 5(a)). The curves represent landslide hazard estimates, and based on them alone, Area A possesses the greatest predicted hazard for the first 23 yr after harvest. However, when the economic information is combined with the hazard estimates to compute time-based EMV's (Fig. 5(b)), Area A is shown to have the greater economic risk (i.e., lesser EMV) only for the first 12.5 yr after harvest.

The EMV values (Fig. 5(b)) for given time periods  $T$  are calculated as follows

$$\text{EMV}(T) = [\text{probability of landslide}(T) \times (\text{timber value} + \text{landslide value})] \\ + [\text{probability of no landslide}(T) \times \text{timber value}] \quad (6)$$

In this manner, quantified estimates of landslide hazard (i.e., probability of slope failure), based on historical precipitation data and a geotechnical slope stability analysis, can be incorporated into risk assessment and decision analysis.

## DISCUSSION AND CONCLUSIONS

A time-based landslide hazard model that incorporates historical precipitation records into probabilistic slope stability analyses can enhance landslide risk assessments. As a result, decision-making practices for resource management and land-use planning are improved. The temporal model is not compre-

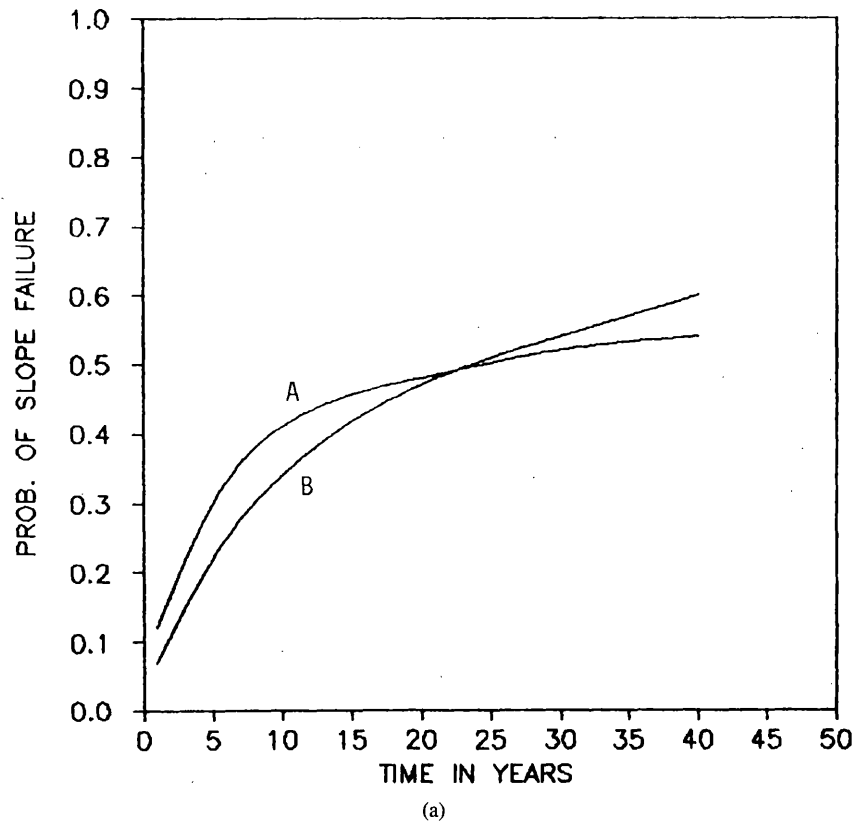


Fig. 5. (a) Probability of slope failure for potential harvest areas A and B. (b) EMV predictions for potential harvest areas A and B.

hensive in that it considers only the nonsteady-state behavior of near-surface groundwater levels and not other factors such as weathering or erosion.

Results from a hazard model based on extreme-value methods must be interpreted carefully. The methods ignore all but the maximum annual values, which may cause some important information to be overlooked. For instance, the maximum annual value may not be unique in a given year, and if this happens more than a few times in the historical record then the predicted hazard will be unreasonably small.

The critical component of the landslide hazard model is the conversion of historical precipitation data to estimates of historical groundwater levels. These estimates provide a catalog of maximum annual water levels that have occurred at a given study site; the maxima are used in an extreme-value analysis to pro-

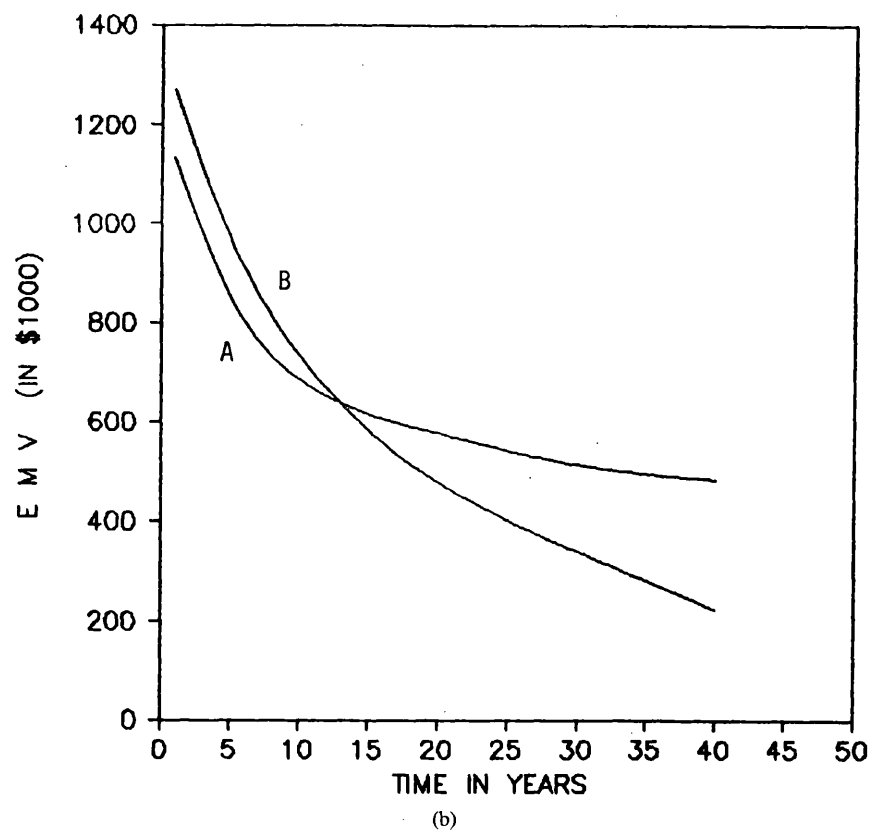


Fig. 5. (Continued)

vide time-dependent cdf's for the maximum annual water levels. Conversion from precipitation to groundwater response is difficult and requires fairly extensive field information from the site. At least 2 yr of groundwater monitoring data are required, preferably from at least three piezometer holes at the site. Sound information on site geology and material properties also is needed, such as depth to bedrock, estimates of hydrogeologic coefficients, and basin drainage characteristics. Additional research and experience are necessary to test current procedures and to determine their limitations. Consequently, the efforts required for a temporal assessment of landslide hazard using current technologies dictate that the project be of major economic or environmental concern. As techniques of near-surface groundwater modeling improve and as more field data and experience are obtained, time-based hazard evaluations for landslides will apply to a greater variety of slope stability investigations.

### ACKNOWLEDGMENTS

Much of the landslide hazard research discussed above was funded by the National Science Foundation, Grant No. ECE-8611573. Valuable technical support was provided by Rod Prellwitz and Carol Hammond, Research Engineers with the U.S. Forest Service Intermountain Experiment Station. Review comments from Richard Pike also were appreciated.

### REFERENCES

- Carr, J. R. and Bailey, R. E., 1986, An Indicator Kriging Model for Investigation of Seismic Hazard: *Math. Geol.*, v. 18, p. 409-428.
- Gumbel, E. J., 1958, *Statistics of Extremes*: Columbia University Press, New York, 375 p.
- Kinnison, R. R., 1985, *Applied Extreme Value Statistics*: Battelle Press, New York, 149 p.
- Kirsten, H. D. and Moss, A. S. E., 1985, Probability Applied to Slope Design—Case Histories, in C. H. Dowding (Ed.), *Rock Masses—Modeling of Underground Openings/Probability of Slope Failure/Fracture of Intact Rock*: ASCE, New York, p. 106-121.
- Miller, S. M., 1984, Probabilistic Rock Slope Engineering: Paper no. GL-84-8: Geotechnical Lab, USAE Waterways Experiment Station, Vicksburg, Mississippi, 75 p.
- Miller, S. M. and Borgman, L. E., 1984, Probabilistic Characterization of Shear Strength Using Results of Direct Shear Tests: *Geotechnique*, v. 34, p. 273-276.
- Neuman, S. P.; Feddes, R. A.; and Bresler, E., 1974, *Finite Element Simulation of Flow in Saturated-Unsaturated Soils Considering Water Uptake by Plants: Hydrodynamics and Hydraulic Engineering Laboratory*, Israel Institute of Technology, Haifa, Israel.
- Newendorp, P. D., 1975, *Decision Analysis for Petroleum Exploration*: Petroleum Publishing Company, Tulsa, Oklahoma, 668 p.
- Prellwitz, R. W. and Babbitt, R. E., 1984, Long-term Groundwater Monitoring in Mountainous Terrain: Paper presented at 63rd Annual Meeting of the Transportation Research Board: Washington, DC, January.
- Prickett, T. A. and Lonquist, C. G., 1971, Selected Digital Computer Techniques for Groundwater Resource Evaluation, *Bull. 55: Illinois State Water Survey*, Urbana, Illinois, 62 p.
- Sangrey, D. A.; Harrop-Williams, K. O.; and Klaiber, J. A., 1984, Predicting Groundwater Response to Precipitation: *Jour. Geotech. Eng. ASCE*, v. 110, p. 957-975.
- Soong, T. T., 1981, *Probabilistic Modeling and Analysis in Science and Engineering*: John Wiley & Sons, New York, 384 p.
- Ward, T. J.; Li, R. M.; and Simons, D. B., 1979, Mathematical Modeling Approach for Delineating Landslide Hazards in Watersheds, in *Proceedings of the 17th Annual Symposium on Engineering Geology and Soils Engineering*: Moscow, Idaho, p. 109-142.